CHAPTER 4

RESULTS AND DATA ANALYSIS

4.1. Identification of the role of ionic liquid $[BMIM]^+[NTf_2]^-$ in the emulsion liquid membrane system

Ionic liquid $[BMIM]^+[NTf_2]^-$ was chosen over other ionic liquids due to its hydrophobicity, minimum toxicity, relatively less viscosity and density. Its physico-chemical properties are, as shown in Table 4.1.

Table 4.1: Physical and thermodynamic properties of $[BMIM]^+[NTf_2]^-$ (Huddleston et al., 2001)

Property	Temperature (°C)	Value
Density (g/ml)	25	1.43
Viscosity (cP)	25	52
Surface tension (dyne/cm) (Water equilibrated[a])	25	36.8
Thermal decomposition temperature (°C) (Water equilibrated[a])		394
Water content (mg/l) (Water equilibrated[a])	25	3280
Melting point(°C) (Dried[b])		4

[a] Water equilibrated denotes that $[BMIM]^+[NTf_2]^-$ was kept in contact with water

[b] Dried stands for water equilibrated $[BMIM]^+[NTf_2]^-$ that was dried at 70 °C for 4 hrs on a vacuum line.

4.1.1. Identification of the role of $[BMIM]^+[NTf_2]^-$ in the emulsion without TOMAC

As the first stage of this study, the role of ionic liquid $[BMIM]^+[NTf_2]^-$ is conjectured to behave as one of the following: either as a carrier, surfactant, solvent or stabilizer. In order to substantiate its role, the following experiments were conducted and are discussed below.

4.1.1.1. Consideration of $[BMIM]^+[NTf_2]^-$ as a carrier

In order to identify the role of $[BMIM]^+[NTf_2]^-$ as a carrier, an emulsion was prepared by using kerosene as solvent, Span 80 as surfactant, NaOH (0.1N) as internal phase and the concentration of $[BMIM]^+[NTf_2]^-$ was varied in the range of 0 – 6% (w/w). I/O ratio was maintained at 1/3 and the concentration of Span 80 was kept 3% (w/w). The initial Cr concentration in the feed phase was 100 mg/L and the pH of the feed was maintained below 1.5. The effect of $[BMIM]^+[NTf_2]^-$ on the percentage removal of Cr in an emulsion liquid membrane is shown in Fig. 4.1. Generally, the role of a carrier in ELM extraction is to enhance the final removal and to increase the rate of extraction. The carrier combines with the desired metal at the outer interface and makes a complex. This complex diffuses through the membrane and reaches the inner interface. At the point, the internal reagent reacts with the complex, converts the metal into a salt which is insoluble in the membrane phase and the carrier diffuses back in the membrane phase. In the absence of TOMAC (carrier), Cr extraction is facilitated by type-I mechanism if $[BMIM]^+[NTf_2]^-$ cannot play the role of a carrier.

If the ionic liquid was presumed to act as a carrier in the emulsion, then the final % removal of Cr and the rate of % removal of Cr should have increased with an increase in the ionic liquid concentration. On the contrary, as illustrated in Fig. 4.1, an increase in concentration of $[BMIM]^{+}[NTf_2]^{-}$ from 0% (w/w) to 2% (w/w) produced an insignificant decrease in the final removal and a significant decrease in the rate of removal can be observed. Moreover, both the parameters kept on decreasing with an increase in the concentration of $[BMIM]^{+}[NTf_2]^{-}$ up to a concentration of 4% (w/w). This indicates that $[BMIM]^{+}[NTf_2]^{-}$ is not involved in making complexes and in transporting the metal from the feed phase to the internal phase. Hence, it's a type-I facilitation where no carrier is present.

Another important observation from the figure is that a maximum removal of Cr (96.5%, in almost 100 minutes) is obtained when there is no $[BMIM]^{+}[NTf_2]^{-}$ and TOMAC in the ELM system.

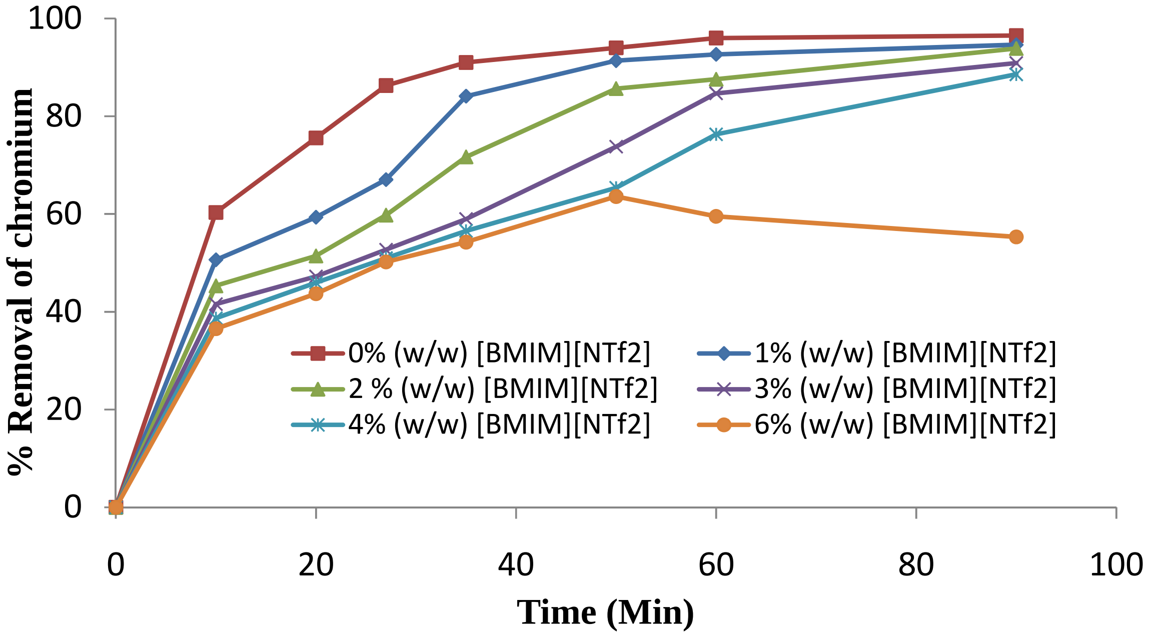

Figure 4.1 The effect of ionic liquid on the extraction of Cr without TOMAC. Span 80 = 3% (w/w); I/O = 1:3 F/E= 2:1

This raises the question of the benefit of using $[BMIM]^+[NTf_2]^-$, when the maximum removal efficiency of 96.5% without any $[BMIM]^+[NTf_2]^-$ or TOMAC. When TOMAC is used as a carrier and $[BMIM]^+[NTf_2]^-$ as a stabilizer then, the time taken for the removal of Cr (~85%) is only around 10 minutes. The reason for using $[BMIM]^+[NTf_2]^-$ with TOMAC has been elaborated in sections 4.1.2 and 4.1.3 of the thesis. Reduction in the time of the operation and an increment in the removal rate minimize the effective energy consumption for the ELM technology.

The decrease in the % removal of chromium with an increase in the concentration of $[BMIM]^+[NTf_2]^-$ can be explained as an increased mass transfer resistance caused by $[BMIM]^+[NTf_2]^-$ during the time of extraction and stripping. It was believed that the diffusion of Cr was hindered by the big size of $[BMIM]^+[NTf_2]^-$. Electrostatic and Vanderwaal's attraction also slowed down the transport of Cr.

A sudden decrease in the % removal of chromium was observed at 6% (w/w) of $[BMIM]^+[NTf_2]^-$ after 50 minutes. This discrepancy can be explicated by the aggregated sedimenting tendency of $[BMIM]^+[NTf_2]^-$ due to its increased weight at higher concentration. It causes the breakage of the membrane and reduces the % removal efficiency of the ELM. From these observations and facts, it can be concluded that $[BMIM]^+[NTf_2]^-$ cannot act as a carrier for this operation.

4.1.1.2. Consideration of $[BMIM]^+[NTf_2]^-$ as a surfactant

The role of a surfactant in the ELM is to minimize the interfacial energy (interfacial tension) between organic and aqueous phases. It not only provides stability to the ELM but also protects globules from high sheer rate and coalescence of droplets. Surfactant properties are dependent on its HLB (hydrophilic-lipophilic balance) number. The head part which is a hydrophilic group stays in the internal aqueous phase and the tail part which is a hydrophobic long carbon chain resides in the membrane phase. As far as ionic liquids are concerned, there is no literature available regarding the use of $[BMIM]^+[NTf_2]^-$ as a surfactant and its HLB number. Hence, interfacial tension of kerosene and NaOH and CMC (Critical Micelle Concentration) of $[BMIM]^+[NTf_2]^-$ were experimentally determined in order to investigate the behaviour of $[BMIM]^+[NTf_2]^-$ as a surfactant. The concentration of $[BMIM]^+[NTf_2]^-$ was varied in the range of 0.4 - 7% (w/w) at the interface of kerosene and NaOH. Interfacial tension remained constant at the value of 30 d/cm for all the concentrations of $[BMIM]^+[NTf_2]^-$ hence, CMC could not be found out. The failure of micelle formation of $[BMIM]^+[NTf_2]^-$ in kerosene can be explained by two possible reasons (Blesic et al., 2007). The first one is the small hydrocarbon tail (butyl) attached to the cationic group of $[BMIM]^+[NTf_2]^-$ does not interact well with hydrocarbon chain of kerosene to form micelles. The second reason that may be attributed is the big size of $[NTf_2]^-$ anion which is hard to fit the micelle surface region (Stern Layer).

Emulsion preparation with kerosene as solvent, NaOH as internal reagent and considering $[BMIM]^+[NTf_2]^-$ as a surfactant was also tried to verify the possibility of emulsion formation. Several combinations of the concentrations of kerosene, NaOH and $[BMIM]^+[NTf_2]^-$ were examined. Emulsion formation didn't take place even under a homogenizer speed of 15000 rpm. Since $[BMIM]^+[NTf_2]^-$ is a hydrophobic ionic liquid and its density is more than kerosene and NaOH, it may not be stable in such colloid system without the help of other stabilizers, and hence emulsion formation failed.

Therefore, it can be concluded that $[BMIM]^+[NTf_2]^-$ does not behave as a surfactant for the above mentioned solvent and internal phase.

4.1.1.3. Consideration of $[BMIM]^+[NTf_2]^-$ as a solvent

Ionic liquids have been proved to be the solvent of the future due to their unique properties over organic solvents. They have already been incorporated in several chemical applications. As far as their usage in the ELM technology is concerned, researchers are investigating their possible role in order to make it less polluted and more efficient. The effect of solvents such as kerosene, toluene, hexane, cyclo-hexane and dodecane has been investigated on the stability and % removal efficiency of the ELM. In order to investigate the feasibility of ionic liquid $[BMIM]^+[NTf_2]^-$ as a solvent for the ELM, the emulsion was prepared using $[BMIM]^+[NTf_2]^-$ as a solvent, Span 80 as a surfactant and NaOH as the receiving phase while keeping the proportions of each component the same as it was prepared with kerosene as a solvent in the previous sections.

The concentrations and volumes of $[BMIM]^+[NTf_2]^-$, Span 80 and NaOH and homogenizing speed and time were varied in order to get a stabilized membrane but the stability lasted only for 5 minutes with the best composition. The density difference between $[BMIM]^+[NTf_2]^-$ and NaOH solution is higher than the difference between kerosene and NaOH therefore, proclivity for sedimentation of the former emulsion is much higher than the latter. Thus, the emulsion formed with $[BMIM]^+[NTf_2]^-$ as solvent lasted only for a short duration.

Another phenomenon that was observed during the process was that the adsorbed amount of Span 80 on the surface of $[BMIM]^+[NTf_2]^-$ was found to be very small. Hence, interfacial tension was not too reduced enough to make fine internal droplets of NaOH. The formation of small droplets of Span 80 takes place on the surface of ionic liquid on increasing the Span 80 concentration above 0.3% (w/w). Another reason for the reduced stability may be explained as the insufficient reduction in interfacial tension of the solvent by Span 80. From the above discussion, it can be concluded that $[BMIM]^+[NTf_2]^-$ cannot be used as a solvent for the above mentioned surfactant and internal phase.

4.1.2. $[BMIM]^+[NTf_2]^-$ as a stabilizer when TOMAC is used as a carrier

As discussed earlier in section 4.1.1.1 that using a carrier in ELM minimizes the energy consumption and saves a lot of time of the process. TOMAC is a very good phase transfer catalyst which is relatively inexpensive, easily available and less toxic over other carriers such as Alamine 336, Aliquat 336, D2EHPA and tributylphosphate (TBP). Therefore, TOMAC was selected as a carrier to study the effect of ionic liquid ($[BMIM]^+[NTf_2]^-$) on the stability of emulsion and subsequent removal efficiency. The problem with TOMAC is that when it is used as a carrier in the ELM with no concentration of $[BMIM]^+[NTf_2]^-$, stability lasted only for 7 minutes (as shown in Fig. 4.2.) which is not sufficient for extraction to take place and for subsequent demulsification.

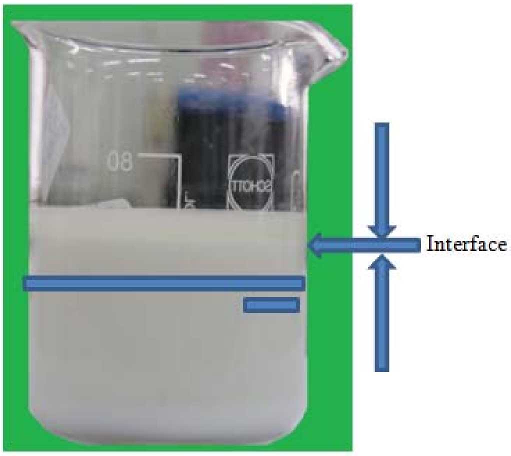

Figure 4.2 Emulsion prepared with 3% (w/w) Span 80, TOMAC =0.29% (w/w); $[BMIM]^+[NTf_2]^-$= 0% (w/w) (after 7 minutes); scale bar =1 cm.

From Fig. 4.3 (a), it can be observed that the emulsion was stable for up to 7 h when 3% (w/w) of the ionic liquid $[BMIM]^+[NTf_2]^-$ was added. On the other hand, Fig 4(b) depicts the separated organic and aqueous phases after 5 h when there was no concentration of $[BMIM]^+[NTf_2]^-$ present in the emulsion. In fact, the phase separation started only after 7 minutes without $[BMIM]^+[NTf_2]^-$ in the emulsion.

The stability time with the varying concentration of $[BMIM]^+[NTf_2]^-$ is shown in Fig. 4.4. The stability time increases with the increase in concentration of $[BMIM]^+[NTf_2]^-$ for up to 3 %(w/w) of $[BMIM]^+[NTf_2]^-$. After 3 %(w/w) of $[BMIM]^+[NTf_2]^-$ onwards, the stability time decreases which consolidates the fact that the $[BMIM]^+[NTf_2]^-$ helps to stabilize the ELM when it is present up to a certain maximum concentration.

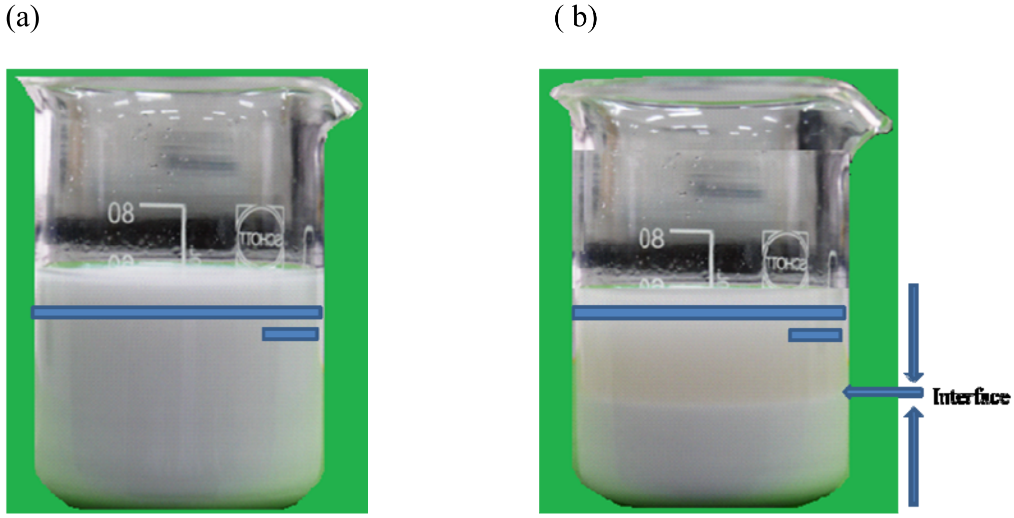

Figure 4.3 (a) Emulsion prepared with $[BMIM]^+[NTf_2]^-$ = 3% (w/w); TOMAC = 0.29% (w/w) (after 7 h) (b) Emulsion prepared with $[BMIM]^+[NTf_2]^-$ = 0% (w/w); TOMAC = 0.29% (w/w) (after 5 h); scale bar = 1 cm.

It was found out that if the ELM contained more than this concentration, emulsion sedimentation took place due to the higher density of the ionic liquid. Each experiment was conducted twice and the results were reproducible with negligible differences between two corresponding values.

Increased stability of the ELM by the addition of $[BMIM]^+[NTf_2]^-$ may be explained by Coulombic interactions of the charges on the ions of ionic liquids $[BMIM]^+[NTf_2]^-$ and TOMAC. The other interactions present in the emulsion were between other chemical complex groups such as Span 80 and TOMAC; TOMAC and NaOH; $[BMIM]^+[NTf_2]^-$ and NaOH etc. These strong interactions helped to avoid the coalescence of the internal droplets, nevertheless it also caused the hindrance to Cr-TOMAC complex diffusion through the membrane.

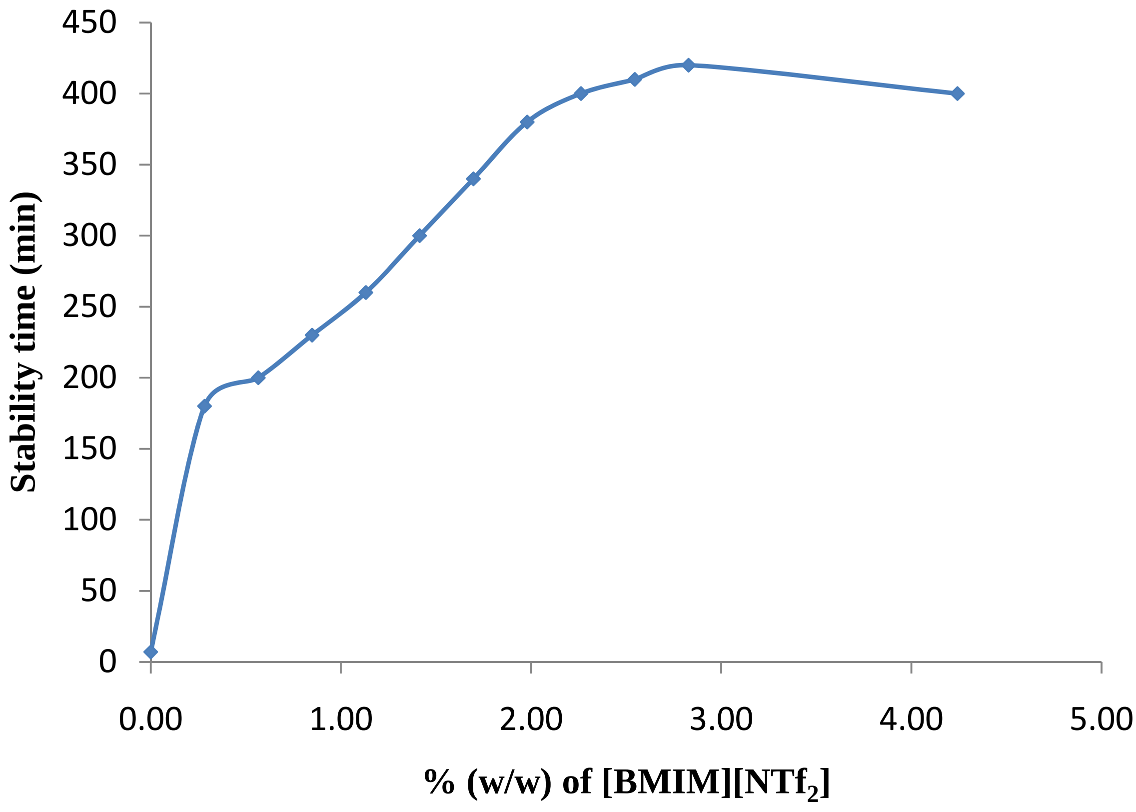

Figure 4.4 The effect of the concentration of $[BMIM]^+[NTf_2]^-$ on the stability time of the ELM. Span 80 = 3 %(w/w); TOMAC = 0.29 %(w/w), I/O =1/3.

Besides strong interactions between ions, there is a possibility of hydrogen bonding present between $[BMIM]^+[NTf_2]^-$ and the $[OH]^-$ group of NaOH. The hydrogen bonding may cause a strong protection surrounding the internal droplets to avoid coalescence. $[BMIM]^+[NTf_2]^-$ is capable of developing a polymeric structure with large cavities when it is used in various kind of reactions (Weingrtner, 2008). These polymeric structures of $[BMIM]^+[NTf_2]^-$ may also help to understand the cause for the enhanced stability. The polymeric structure of $[BMIM]^+[NTf_2]^-$ may behave like polymeric surfactant of the A–B, A–B–A or $(BA)_n$ graft type to generate a repulsive barrier to prevent the collapse of the ELM and forestall the sedimentation.

4.1.3. Effect of $[BMIM]^+[NTf_2]^-$ concentration on phase separation rate of the stabilized emulsion

The emulsion was prepared with kerosene as solvent, Span 80 as surfactant, NaOH (0.1N) as internal phase, TOMAC as carrier and varying amount of $[BMIM]^+[NTf_2]^-$. I/O ratio was maintained at 1/3 and Span 80 concentration was kept 3% (w/w). TOMAC concentration was kept at a constant value of 0.29% (w/w). The emulsion started to separate into organic and aqueous phases after achieving maximum stability time which is dependent on the concentration of the ionic liquid. Creaming and coalescence are the main causes for emulsion sedimentation for the current composition of emulsion. Sedimentation of the emulsion due to Ostwald ripening was insignificant since, aqueous NaOH and kerosene are almost insoluble in each other.

The stabilized membrane was held for the next 3 h after it starts to destabilize to analyze the stability of it with respect to the concentration of $[BMIM]^+[NTf_2]^-$. The calculation of the phase separation was done by noting the height of the interface from the bottom of the beaker at regular intervals.

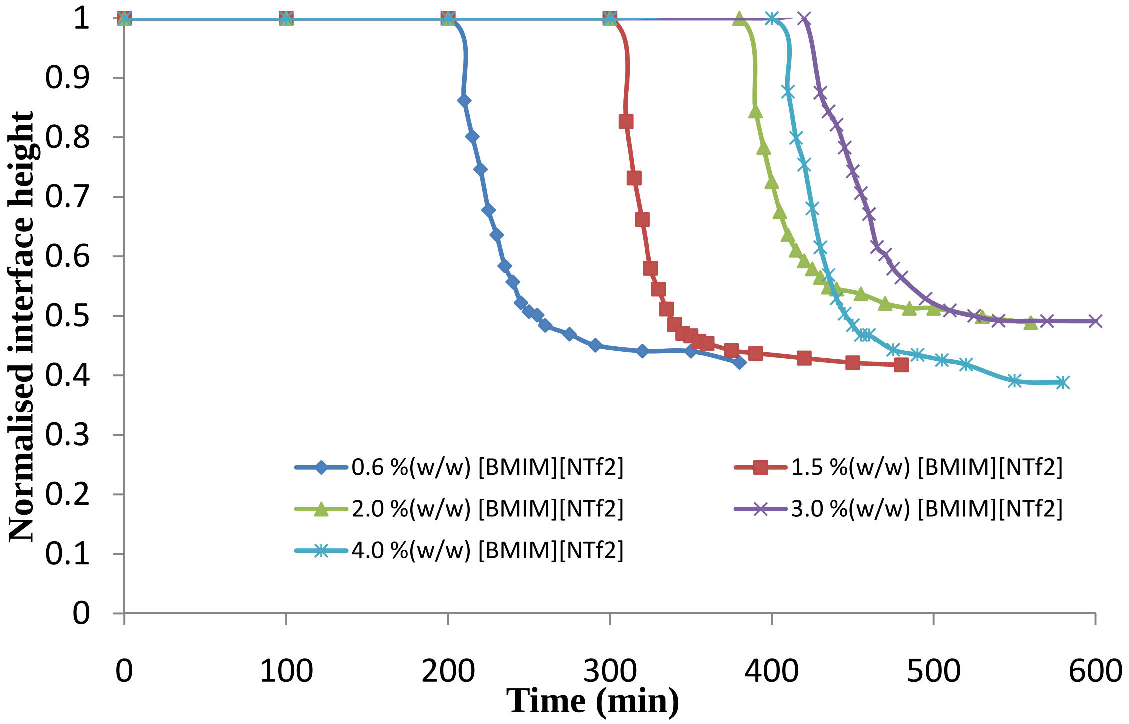

Figure 4.5 The effect of ionic liquid concentration on the phase separation of the stabilized membrane. TOMAC = 0.29% (w/w); Span 80 = 3% (w/w); I/O = 1:3

The stabilized membrane stability time and their phase separation with respect to time are shown in Fig. 4.5. It can be observed from Fig. 4.5 that increasing the concentration of $[BMIM]^+[NTf_2]^-$ to 3% (w/w) increases the final (after 3 h) interface height of the destabilized emulsion. It implies that the sedimentation rate decreases with an increase in the concentration of $[BMIM]^+[NTf_2]^-$, up to 3% (w/w). The decreased sedimentation rate may be explained by the effective electrostatic interactions between the two ionic liquid; $[BMIM]^+[NTf_2]^-$ and TOMAC, over the density of ionic liquids and NaOH. Fig. 4.5 also illustrates an increment in the concentration of $[BMIM]^+[NTf_2]^-$ above 3% (w/w) decreases the interface height of the destabilized emulsion which means that the sedimentation rate of the destabilized emulsion increases upon increasing the concentration of $[BMIM]^+[NTf_2]^-$ above 3% (w/w). The increased sedimentation can be accounted by the dominance of the density of $[BMIM]^+[NTf_2]^-$ and NaOH over electrostatic interactions between ionic liquids $[BMIM]^+[NTf_2]^-$ and TOMAC. However, the complete phase separation of the stabilized membrane into its original phases was observed only after 2-3 days.

4.1.4. The removal efficiency of the emulsion liquid membrane stabilized by ionic liquid $[BMIM]^+[NTf_2]^-$ with TOMAC

The emulsion was prepared with the concentration of $[BMIM]^+[NTf_2]^-$ in the range of 0.6 – 4.0% (w/w) and TOMAC concentration was kept at a constant value of 0.29% (w/w). The prepared emulsion was kept for 2 hrs to verify its stability. Subsequently, it was poured into an unbaffled beaker containing Cr feed phase under an agitation of 300 rpm provided by a mechanical stirrer. The samples were taken at regular intervals.

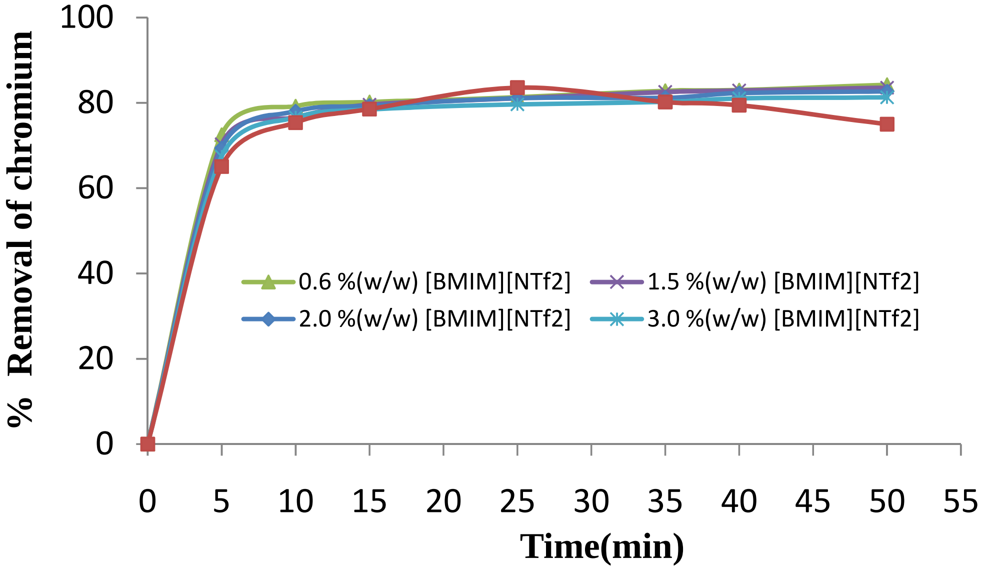

Figure 4.6 The effect of ionic liquid concentration on the extraction of Cr with TOMAC as a carrier. TOMAC = 0.29% (w/w); Span 80 = 3% (w/w); I/O = 1:3; F/E= 2:1

The effect of ionic liquid $[BMIM]^+[NTf_2]^-$ on the removal efficiency of the emulsion liquid membrane having TOMAC as a carrier is shown in Fig. 4.6. It can be seen from the figure that increasing the concentration of $[BMIM]^+[NTf_2]^-$ merely affects the % removal of Cr. It further consolidates the fact that ionic liquid $[BMIM]^+[NTf_2]^-$ does not play any role as a carrier. On the contrary, the % removal of the ELM decreases slightly due to the hindrance caused by both of the compounds i.e. $[BMIM]^+[NTf_2]^-$ and TOMAC. The figure shows that the time taken for 70% of the removal of Cr is only 5 minutes and on the other hand, it was more than 50 minutes for the emulsion without any concentration of TOMAC and $[BMIM]^+[NTf_2]^-$. Hence, both the extraction time and the effective cost of operation could be reduced by a substantial amount by using TOMAC and $[BMIM]^+[NTf_2]^-$. Since the ELM technology compromises with its stability in industrial scale operations, the usage of ionic liquid $[BMIM]^+[NTf_2]^-$ might help to overcome not only the stability problem but also the environmental issues. However, the microscopic studies such as globules and internal droplet sizes, change in the globule size with respect to time and properties of TOMAC and $[BMIM]^+[NTf_2]^-$ and characterization of the stabilized emulsion remain areas to be explored.

4.1.5. Stability time determination in terms of $[BMIM]^+[NTf_2]^-$ concentration and initial rate of sedimentation

The experimental data of stability time and the initial rate of sedimentation of the emulsion prepared with TOMAC = 0.29% (w/w); Span 80 = 3% (w/w); I/O = 1:3 is given in Table 4.2.

Table 4.2: Experimental data on stabilized time with ionic liquid concentration $[BMIM]^+[NTf_2]^-$ and initial rate of sedimentation height with TOMAC = 0.29% (w/w); Span 80 = 3% (w/w); I/O = 1:3.

Concentration of $[BMIM]^+[NTf_2]^-$ (%w/w)	Initial rate of sedimentation (min^{-1})	Experimental stability (min)
0.6	0.0150	220
1.5	0.0120	330
2.0	0.0100	400
3.0	0.0086	425
4.0	0.0067	465

The stability time of the emulsion as a function of $[BMIM]^+[NTf_2]^-$ concentration (%w/w) (x_1) and initial rate of sedimentation (x_2) are correlated as follows:

$$t_{s,\,pred} = a x_1^{b} x_2^{c} + 7 \text{ where a, b and c are parameters} \tag{1}$$

The term 7 minutes in the above correlation indicates the stabilized time when the concentration of $[BMIM]^+[NTf_2]^-$ is equal to zero in the ELM containing TOMAC as carrier, NaOH as stripping phase and kerosene as solvent. The parameters are estimated using data in Table 1 by nonlinear parameter estimation scheme with the help of MATLAB 7.0.4 software and the predicted stabilized time relationship is given as

$$t_{s,\,pred} = 1446.6 x_1^{0.54549} x_2^{0.38057} + 7 \tag{2}$$

Table 4.3: Comparison between experimental stability time and predicted stability time.

Concentration of $[BMIM]^+[NTf_2]^-$ (% w/w)	$t_{s, exp}$ (min)	$t_{s, pred}$ (min)	% deviation
0.6	220	221.4	0.6
1.5	330	335.3	1.6
2.0	400	365.9	8.5
3.0	425	430.5	1.3
4.0	465	457.7	1.5

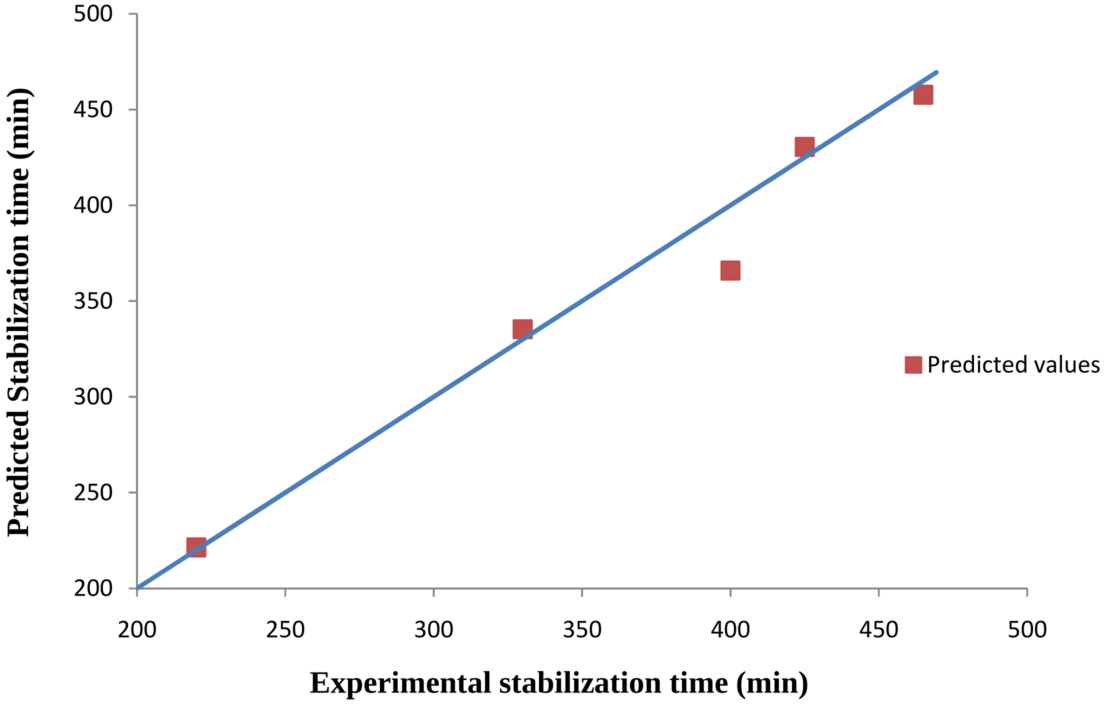

Figure 4.7 Experimental stability time versus predicted stability time.

The stability time of emulsion depends more on the concentration of $[BMIM]^+[NTf_2]^-$ than on the initial rate of sedimentation of the emulsion as observed from eq. 2. The comparison between the predicted values and experimental values is reported in Table 4.3.

The low values of deviation as summarized in Table 4.3 imply the accuracy of the correlation. The predicted and experimental stabilized times are in good agreement within ± 9% deviation, as shown in Fig. 4.7. However, the correlation is only applicable for lower ranges of the $[BMIM]^+[NTf_2]^-$ concentrations. It does not hold the accuracy for higher concentrations of ionic liquid $[BMIM]^+[NTf_2]^-$.

4.2. Parameter optimization for $[BMIM]^+[NTf_2]^-$ stabilized emulsion liquid membrane extraction process

The performance of the ELM technology is dependent on the properties of a number of components such as carrier, surfactant, solvent, stabilizer, internal phase homogenization speed and agitation speed. Each element affects the final removal efficiency in its own way. The other important process parameters are the pH of the receiving phase and feed phase, the ratio of the feed to emulsion phase ratio (F/E) and the ratio of the internal to organic phase (I/O). Hence, the ELM process parameters optimization becomes necessary to obtain the maximum removal of chromium.

The effects of the parameters were determined by calculating the final % removal of Cr in the feed phase. One parameter was varied in a certain range while others were kept constant. The concentration of $[BMIM]^+[NTf_2]^-$ was kept constant at 3% (w/w) in every experiment in order to gain the maximum stability of the ELM. The results are described in the following subsections.

4.2.1. Effect of internal phase concentration

As mentioned earlier, the pH difference between the feed phase and the internal phase is the main driving force to transport the solute-carrier complex (H_2CrO_4.TOMAC) through the membrane phase. Since NaOH is the internal phase reagent in the ELM system, its concentration directly affects the pH of the internal phase. Increasing the Molarity of the internal aqueous phase (NaOH) increases the pH of the internal phase that generates a pH gradient between the feed phase and the internal phase. Consequently, the rate of solute-carrier complex formation increases at the outer interface.

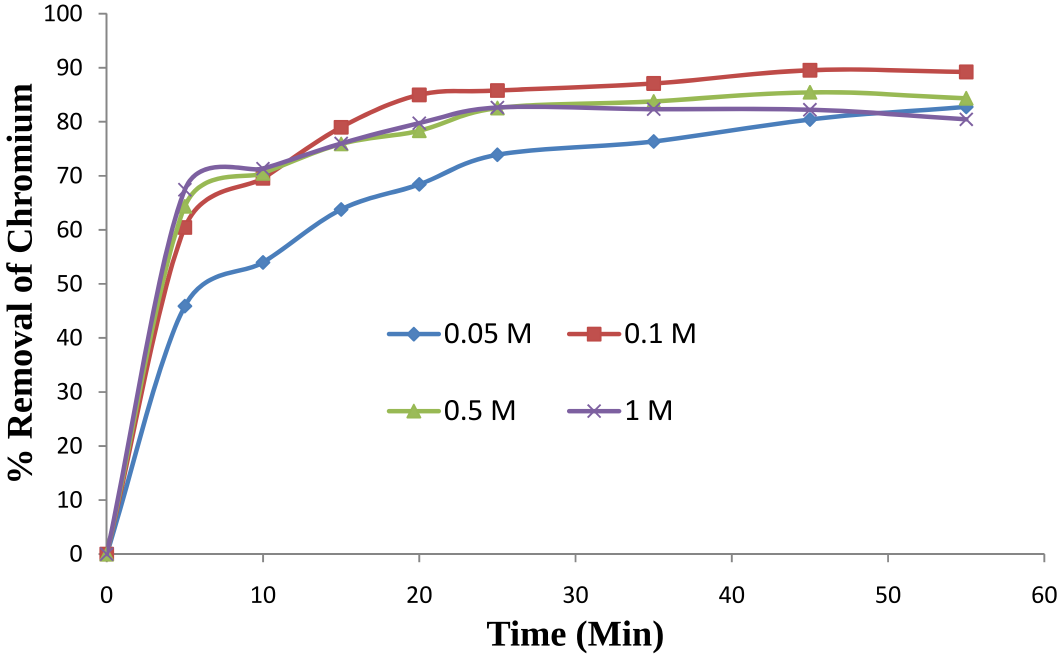

Figure 4.8 The effect of internal phase concentration. TOMAC = 0.29% (w/w); Span 80 = 3% (w/w); I/O = 1:3; $[BMIM]^+[NTf_2]^-$= 3% (w/w); F/E= 2:1; agitation speed = 300 rpm.

Similar results are obtained upon increasing the concentration of NaOH in the internal phase, as shown in Fig. 4.8. An increment in the concentration of NaOH from 0.05M to 0.1M increased the final percentage removal because more solute-carrier complex travelled through the membrane. Moreover, an increment in NaOH concentration increases the stripping rate of Cr since there are more $[OH]^-$ groups at the inner interface to react with solute-carrier complex.

However, a further increase in NaOH concentration reduces the final percentage removal of chromium as indicated in Fig. 4.8. The results show that a change in NaOH concentration from 0.1 to 0.5 M leads to a decrease of 5% in the removal efficiency. It was showed a further decrease upon increasing the concentration of NaOH up to 1M. This implies that % removal efficiency attains an optimum at value of 0.1 M of NaOH concentration and after which it starts to decline. The plausible explanations for this behaviour are as follows:

- NaOH had a tendency to react with Span 80 and $[BMIM]^+[NTf_2]^-$ that became prominent with an increase in concentration of NaOH. NaOH might have modified the properties of Span 80 and $[BMIM]^+[NTf_2]^-$ by forming other compounds (Chiha et al., 2006). As a result, the effective number of Span 80 and $[BMIM]^+[NTf_2]^-$ molecules decreased and the stability of the ELM decreased. This caused a breakage of the ELM and the stripped solute diffused back to the feed phase thereby reducing the effective removal efficiency of the ELM.

- Yet, another reason for the depleted removal efficiency with an increase in NaOH concentration can be given as the increased difference in osmotic pressure between the feed phase and the internal phase. Ultimately, it caused membrane swelling which diminished the amount of final recovery (Chakrabarty et al., 2010).

- As NaOH concentration increased, the inner interface started to saturate with the sudden increase in the number of (H_2CrO_4-TOMAC) complex. This saturation decreased the driving force for the solute-complex formation. Therefore, the rate of extraction decreased (Kumbasar, 2008).

The optimum concentration of NaOH was found to be 0.1 M in order to get the maximum removal of Cr. For this reason, it was selected as the required concentration for the further experiments.

4.2.2. Effect of Carrier concentration

Carrier concentration and its characteristics play a vital role in the extraction of metal ions in Type-II facilitation. The extraction of a metal depends on the selectivity of a carrier. The purpose of this study was to obtain an optimum value for the concentration of the carrier TOMAC in order to achieve the maximum removal efficiency. The economy of the ELM process is highly dependent on the amount of carrier used.

The effect of a carrier on the removal efficiency is dependent on how easily it makes a complex with the metal ion and also on the rate of the stripping reaction at the inner interface. Shiau and Jung (1993) demonstrated that an increment in the concentration of a carrier (LIX 64N) increased the selective separation of Cd and Zn from a mixture of Cd, Ni and Zn. On the other hand, the selective separation of Cd and Zn was unaffected by the concentration of a carrier (LIX 64N) due to the close equilibrium values of both the metals with the carrier.

Kulkarni et al. (2002) reported that increasing the concentration of carrier (TOPO) increases the extraction rate of Uranium (VI) at the outer interface but also simultaneously reduces the stripping rate due to the saturation of the inner interface by the solute-carrier complex. Raghuraman et al. (1994) accounted that the extraction of Zn was unaffected by the variation in the concentration of carrier (D2EHPA). They rationalized it as the simultaneous extraction and stripping in a coarse emulsion that helps to keep the loading of solute-carrier complexes low in the membrane phase. Therefore after a certain concentration of the carrier, the final removal of Zn remains unaffected by further addition of D2EHPA. It implies that the extraction reaction at the outer interface is not rate controlling.

Nevertheless, in the present system it was witnessed that TOMAC concentration affected the final percentage removal of Cr by a substantial amount. The concentration of TOMAC was varied in the range of 0.1 – 0.5% (w/w) and the final % removal is, as shown in Fig. 4.9. It can be observed from Fig. 4.9 that increasing the concentration of TOMAC increases the final removal efficiency up to a value of 0.3% (w/w) of TOMAC concentration. This can be explained by the enhanced number of reactions at the outer interface. An increased number of solute-carrier complexes travelled through the membrane phase and reacted with the receptor (NaOH) present in the internal phase. Consequently, the amount of metal stripped increased hence, % removal. At an optimum concentration, 92% of Cr could be removed.

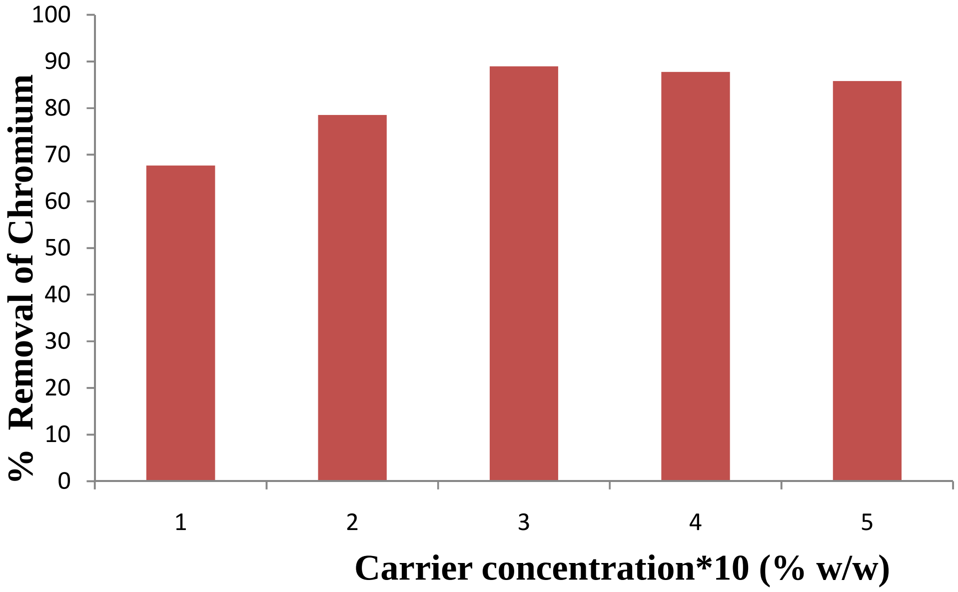

Figure 4.9 The effect of carrier concentration. [NaOH] = 0.1 M; Span 80 = 3% (w/w); I/O = 1:3; $[BMIM]^+[NTf_2]^-$= 3 %(w/w); F/E= 2:1; agitation speed = 300 rpm.

A slight decrement was observed when the concentration of TOMAC was increased from 0.3 to 0. 4% (w/w) and it remained almost constant with a further increase in the concentration. This is caused by a saturation of the inner interface. An increase in the concentration of TOMAC above 0.3% (w/w), the number of unstripped solute-carrier complex increases. This led to the decrease in the stripping reaction rate. So, the final removal decreases. Similar results were reported by Kumbasar et al. (2009) for the extraction of Cr using TOPO as an extractant.

The % removal of chromium with different concentration of TOMAC during the whole extraction process is illustrated in Fig. 4.10. It indicates that the % removal increases with the increment in the concentration of TOMAC for a particular time. This is due to a large number of solute-carrier complexes travelled through the membrane phase and were stripped at the inner interface.

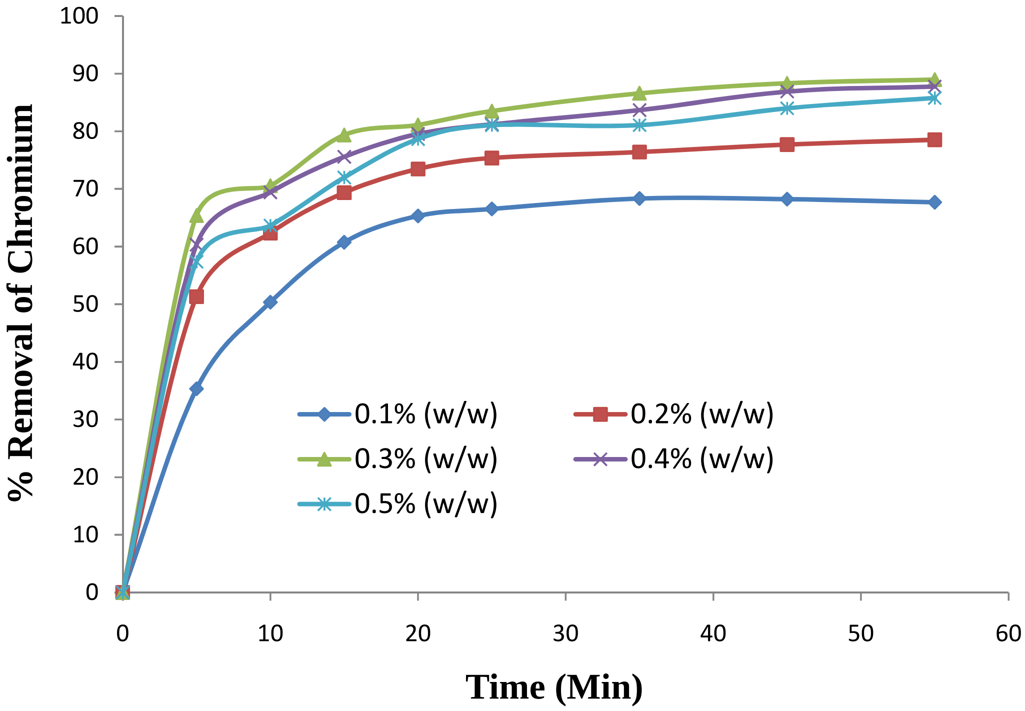

Figure 4.10 The effect of extractant (carrier) concentration. [NaOH] = 0.1 M; Span 80 = 3% (w/w); I/O = 1:3; $[BMIM]^+[NTf_2]^-$= 3% (w/w); F/E= 2:1; agitation speed = 300 rpm.

Another important effect of the carrier concentration which is noticed is that it decreased the viscosity of the membrane phase which directly enhanced the rate of mass transfer of the solute-carrier complex. Thus, the rate of extraction increased with an increase of TOMAC concentration. Further increment in the concentration of TOMAC reduced the viscosity of the membrane by a significant amount which caused negative repercussions in the stability of the membrane. Similar kind of effects can be observed from Fig. 4.10

From the result and discussion, the optimum value for the carrier was achieved to be 0.3% (w/w). Though, a lower concentration of carrier is preferred this compromises the final removal efficiency. So, a value of 0.3% (w/w) was chosen for further experiments.

4.2.3. Effect of Surfactant concentration

Emulsion stability is considered as “Achilles heel” of the ELM process (Abou-Nemeh and Van Peteghem, 1992). The performance of the ELM is directly proportional to the stability of the ELM during the time of extraction. ELMs are very thin, mobile and are subject to shear. They are inclined to be torn during the extraction process. The three factors on which the stability of the ELM depends are as follows:

- internal droplet size (Frankenfeld et al.,1981)
- the shear produced by agitation (Stroeve and Varanasi, 1984)
- composition of the membrane (Stroeve and Varanasi, 1984)

The composition of ELM plays a vital role to determine the stability of the ELM and it can be manipulated in order to improve its efficiency. An increase in surfactant concentration and membrane viscosity have been reported as two remedies to enhance the stability of ELM (Skelland and Meng, 1999).

Surfactants are adsorbed at the inner interface with their hydrophilic part in the internal phase and the lipophilic part in the membrane oil phase. They reduce the interfacial energy of the droplets and make a protective layer surrounding the internal droplets. This layer protects them from coalescence and shear stress and it stabilizes the membrane. On the other hand, surfactant concentration also changes the viscosity and the mass transfer resistance of the ELM (Shen et al., 1996).

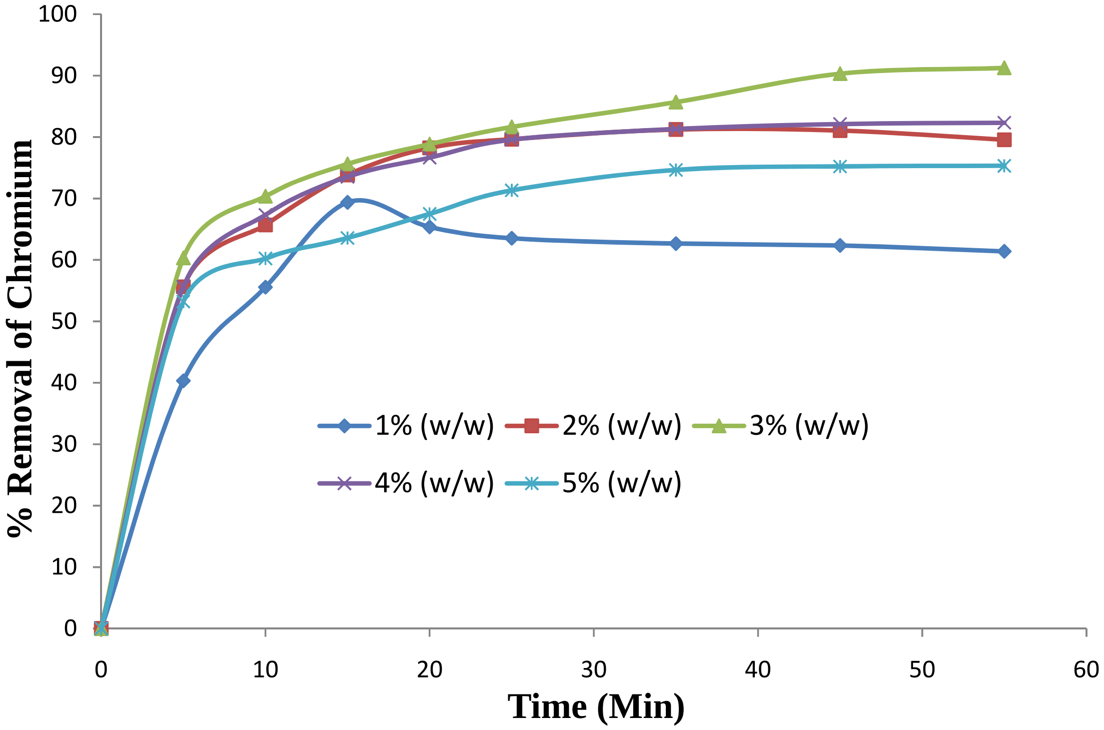

Figure 4.11 The effect of surfactant concentration. [NaOH] = 0.1 M; [TOMAC] = 0.3 %(w/w); I/O = 1:3; $[BMIM]^{+}[NTf_2]^{-}$= 3 %(w/w); F/E= 2:1; agitation speed = 300 rpm.

The effect of Span 80 concentration on the percentage removal efficiency is depicted in Fig. 4.11. As it was expected, the percentage removal efficiency increases with an increase in Span 80 concentration up to 3% (w/w) due to the enhanced stability of the membrane. The leakage from the internal phase was found to be decreasing with an increase in the concentration of Span 80. A concentration lower than 3% (w/w) for Span 80 was not enough to surround the internal droplets completely, and hence interfacial energy was not reduced to the desired value. Consequently, droplets coalesced with each other which ruptured the membrane. Breakage in the membrane allowed the metal salt to diffuse from the internal phase to the external phase.

Further increase in the concentration of Span 80 had three negative effects on the performance of the ELM:

1. The viscosity of the ELM increased upon increasing the concentration of Span 80 which not only increased the stability of the membrane but also increased the mass transfer resistance for the diffusion of the metal-carrier complex. Thus, the % removal of Cr decreased.
2. After a certain value of Span 80, micelles formation in the membrane phase took place. Micelles are considered as precursors to membrane swelling. Reverse micelle encapsulated water molecules in its core diffused through the membrane phase and were finally released in the internal phase (Skelland and Meng, 1996). Ultimately, the water content in the internal phase kept on increasing until the emulsion broke down. It also contributed in the decrement of the % removal of Cr.
3. Solvation of the surfactant molecules by the feed phase. In this case, the surfactant molecules lost their identity and the effective number of surfactant molecules surrounding the internal droplet decreased. Therefore, the stability of the membrane decreased and the % removal efficiency decreased.

It can be deduced that by using a high amount of Span 80, the swelling and stability of the membrane can easily decrease and increase respectively. Nonetheless, both of the parameters were compromised with an increment in mass transfer resistance and an increment in viscosity. Apart from mass transfer resistance and viscosity, a higher amount of surfactants make the de-emulsification and metal recovery difficult from the stripped phase.

The surfactant concentration was kept at a value of 3% (w/w) for the forthcoming experiments.

4.2.4. Effect of agitation speed

Like the composition of the ELM plays an important role in the removal of Cr, similarly the hydrodynamics of the reactor influences the recovery by a substantial amount. Hydrodynamics of the reactor includes agitation speed, impeller blade size and the position of the impeller in the W/O/W double emulsion. The latter two have been found to have an insignificant effect but the former has an important impact on the % removal of Cr.

The concentration of stripped Cr depends on the rate of formation of the Cr-TOMAC complex at the outer interface. Apparently, the rate of formation of Cr-TOMAC is directly proportional to the available surface area of the emulsion globules. If the sizes of the emulsion globules are smaller then, the available surface area increases. Accordingly, the rate of formation of the complex increases. By agitation, energy is transferred to the emulsion which is converted into different sizes of emulsion globules. The transferred energy remains on the surface of the globules as interfacial energy. This energy makes the surface molecules (carrier in this case) more energetic to react with the solute molecules. A different way to understand this phenomenon is that as the size of the emulsion globule decreases, the chemical potential of the droplet increases (Gibbs-Thomsan relation; $\mu \propto 1/r$) where, μ is the chemical potential and r is the radius of a globule. Mass transfer rate also increases with an increase in the surface area of the emulsion globules.

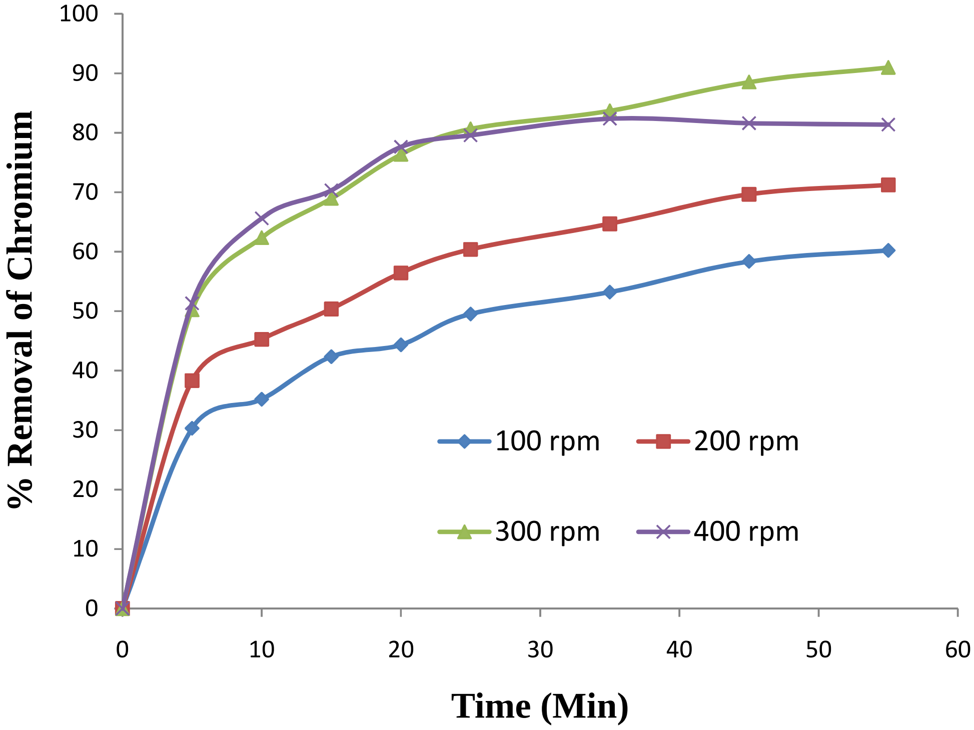

Figure 4.12 The effect of agitation speed. [NaOH] = 0.1 M; Span 80 = 3 %(w/w); [TOMAC] = 0.3 %(w/w); I/O = 1:3; $[BMIM]^+[NTf_2]^-$= 3 %(w/w); F/E= 2:1.

Fig. 4.12 depicts similar effects as discussed above for instance, as the final % removal of chromium increases, the agitation speed of the mechanical stirrer increases for an agitation speed up to 300 rpm. Nonetheless, a further increase in the agitation speed reduces the final removal of Cr. It should be noted from Fig. 4.12 that until 40 minutes the trends of 300 rpm and 400 rpm are almost similar and the removal by 400 rpm was greater than 300 rpm till 30 minutes. Although, after 40 minutes, a sudden decrease in the removal can be seen for 400 rpm. This can be explained as the breakage of the emulsion due to high shear stress for a long time. High shear rate ruptured the globules and the stripped Cr diffused to the feed phase. Swelling is another parameter that may affect the efficiency negatively when the agitation speed is increased. An increase in the agitation speed increased the rate of water molecules transfer through the membrane with the help of reverse micelles or surfactants. The membrane swelled due to the entrance of a large amount of water molecules in the internal phase. As a result, the membrane was ripped open and all the stripped Cr diffused to the feed phase.

Conclusively, 300 rpm was found to be the best agitation speed for the present system. This was deduced after the trade-off between two opposite effects (as described above) was considered.

4.2.5. Effect of treat ratio (Feed phase to emulsion liquid membrane phase)

Treat ratio is defined as the volume ratio of the feed phase to the ELM phase. It determines the effectiveness and the economy of the ELM process. A least volume of the ELM is favoured such that the process is cost effective over solvent extraction. The treat ratio was varied in the range of 1-3 by changing the volume of the feed phase and keeping the volume of the ELM phase constant.

An increase in the treat ratio resulted in a decrement in the volume of the membrane. This reduced the probability of the swelling and the breakage of the ELM. The effective concentration of Cr per globule increased which enhanced the rate of extraction of Cr at the outer interface. The results show that after a certain period of time (20 minutes) the final percentage removal is unaltered with respect to time, as shown in Fig. 4.13. This can be explained due to the saturation of the inner interface. The saturation occurred due to the higher rate of extraction as compared to the rate of stripping. The best result for the removal of Cr was obtained for at a value of 2 for the treat ratio and about 92% of the Cr was removed from the feed phase.

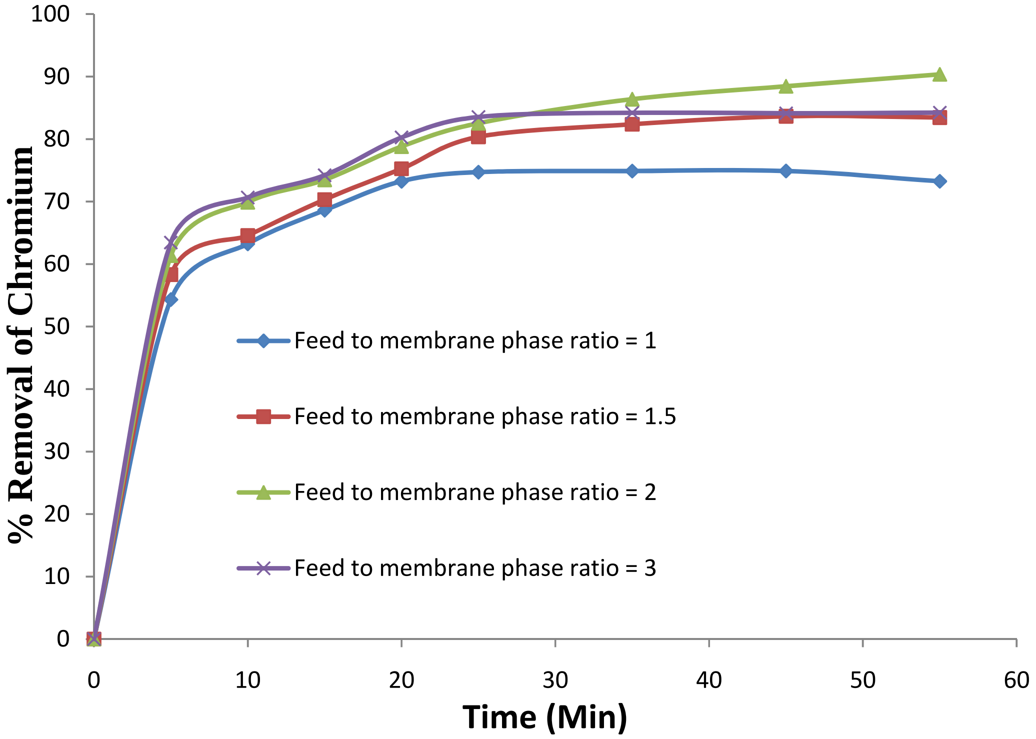

Figure 4.13 The effect of treat ratio. [NaOH] = 0.1 M; Span 80 = 3 %(w/w); [TOMAC] = 0.3 %(w/w); I/O = 1:3; $[BMIM]^+[NTf_2]^-$= 3 %(w/w); agitation speed = 300 rpm.

However, a further increase in the treat ratio affects the final removal efficiency negatively as shown in Fig. 4.13. For example, the rate of removal of Cr increases up to 30 minutes at a treat ratio value of 3. After 30 minutes, an abrupt decline in the removal efficiency occurs. This could be attributed to an increment in the swelling of the membrane due to the large amount of water molecules present in the feed phase. Another feasible reason for this phenomenon is that there was no more internal reagent left in the internal phase to react with the transported complex. As a result, the carrier concentration at the outer interface decreased and the extraction rate decreased but the swelling process remained unaffected. Subsequently, the membrane ruptured which increased the concentration of the feed phase.

Treat ratio also measures the emulsion holdup in the system i.e. it calculates the volume of the ELM required per unit volume of the feed phase. The success of the ELM process depends on the minimized value of the volume of the ELM for the treatment of a definite volume of the feed phase. Unfortunately, the volume of the ELM can be decreased up to a certain extent after which it was compromised with the final removal. Basically, it determines how effectively it can be used on an industrial scale. A treat ratio with a value of 2 was found to be most economical and efficient for the removal of Cr. Therefore, this value has been selected for further studies.

4.2.6. Effect of pH of the feed phase

The pH difference between the feed phase and the internal phase is one of the driving forces for the diffusion of solute-carrier complex molecules through the membrane phase. Hence, the pH of the feed phase plays an important role in the % removal of Cr. The pH of the feed phase can be adjusted with different kinds of acids such as HNO_3, HCl and H_2SO_4. Kumbasar (2009) suggested that the adjustment of the pH of the feed phase by HCl acid results in better removal of Cr than HNO_3 and H_2SO_4. It not only enhances the removal of Cr but also maintains the stability of the membrane for a longer period. Hence, HCl acid was used to set the pH of the feed phase.

Chromate ions exist in various forms in aqueous phase such as $HCrO_4^{-}$, CrO_4^{2-}, $Cr_2O_7^{2-}$ and $HCr_2O_7^{-}$. The total amount of chromium and the pH of the feed phase dictate the prevailing species present in the feed phase. In basic or slightly acidic medium, CrO_4^{2-} ion exists as a dominant species. On the other hand, $Cr_2O_7^{2-}$ was found to be the most prevailing ion in an acidic aqueous phase. However, when the concentration of Cr lies in the range of $(1.26–1.74)\times10^{-5}$ mol/m^3 in an acidic aqueous phase then, $Cr_2O_7^{2-}$ converts in to $HCrO_4^-$ (Bhowal and Datta, 2001). Therefore, chromate ions will exist as $HCrO_4^-$ in the feed phase at low initial concentration of 100 - 500 ppm of Cr(VI).

When TOMAC is used as an extractant or as a carrier then, it also reacts with the internal reagent (NaOH). Thus, there are two types of extractants present in the membrane phase; one is TOMAC and the other is TOMAOH. Both of the extractants react with $HCrO_4^-$ to form a complex as shown in the Reactions 1 and 2

$$\mathrm{TOMAOH} + HCrO_4^- \Leftrightarrow \mathrm{TOMAHCrO_4} + OH^- \qquad (1)$$

$$\mathrm{TOMAC} + HCrO_4^- \Leftrightarrow \mathrm{TOMAHCrO_4} + Cl^- \qquad (2)$$

This complex diffuses through the membrane to the inner interface where it is stripped by an internal reagent and yields $HCrO_4^-$ ion and the extractant. Since, chloride ions are also present in the internal phase from the reaction between TOMAC and NaOH, they also help to strip the complex. Once the complex gets dissociate into $HCrO_4^-$ ion and carrier, the $HCrO_4^-$ ions remain in equilibrium with $Cr_2O_7^{2-}$ after reacting with the OH^- group as shown in Reaction 3.

$$HCrO_4^- + OH^- \Leftrightarrow CrO_4^{2-} + H_2O \qquad (3)$$

As the extraction proceeds forward with time, the pH of the external phase keeps on increasing. The acidic feed phase starts to turn into a basic medium. Consequently, $HCrO_4^-$ converts into CrO_4^{2-} ions. CrO_4^{2-} ions react slowly with TOMAC or TOMAOH to form a complex. Each CrO_4^{2-} species requires two carriers which either comes from TOMAC or TOMAOH or one from each to make a complex. Therefore, the rate of the extraction of Cr keeps on decreasing with time.

During the study, the investigators found that there should be a minimum amount of concentration of [H$^+$] or the pH for the extraction to take place. If the concentration of [H$^+$] was lower than the minimum [H$^+$] concentration or pH was higher than the required pH then, the % removal of chromium would be insignificant.

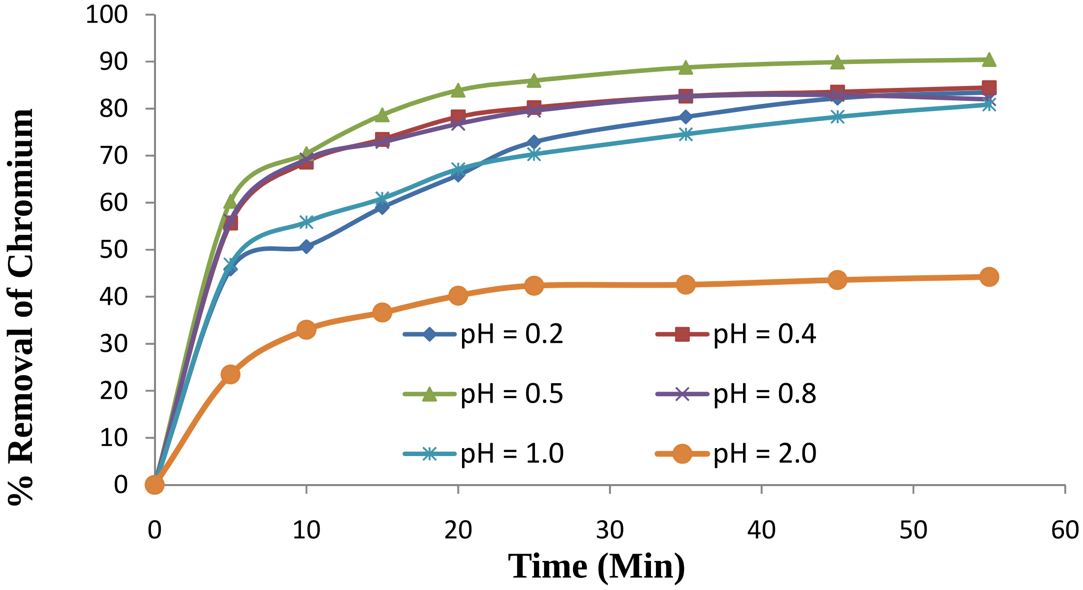

Figure 4.14 The effect of pH of the feed phase. [NaOH] = 0.1 M; Span 80 = 3 %(w/w); [TOMAC] = 0.3 %(w/w); I/O = 1:3; [BMIM]$^+$[NTf$_2$]$^-$= 3 %(w/w); agitation speed = 300 rpm; F/E = 2:1.

The pH of the feed phase was varied in the range of 0.2 to 2.0. Results are as exhibited in Fig. 4.14. To understand the effect of the pH on the % removal of Cr, moving from the higher value of pH to the lower value of pH, only 42% removal could be achieved when the value of the initial pH was 2 as shown in Fig. 4.14. This can be explained by the fact described above i.e. CrO_4^{2-} ions prevailed at a higher value of pH of the feed phase. As a result, the complex formation rate declined by a significant amount.

When the pH of the feed phase was varied from 1 to 0.5, the [H$^+$] ions and $HCrO_4^-$ ions increased simultaneously in the feed phase. CrO_4^{2-} ions were converted into $HCrO_4^-$. The number of $HCrO_4^-$ ions increased by a large amount. The rate of the formation of the complex increased with the increase in the number of $HCrO_4^-$ ions. Subsequently, the rate of removal increased. This trend continued until a pH value of 2.

Nevertheless, a further increase in $[H^+]$ concentration or decrease in pH was observed to reduce the % removal efficiency of the ELM. It can be explained by two simultaneous phenomenons.

On increasing the concentration of $[H^+]$ ions in the feed phase, $[H^+]$ ions reacted with $HCrO_4^-$ ions and yielded the compound H_2CrO_4, as shown in reaction 4. This compound may not be ionized to form a complex with the carrier.

$$HCrO_4^- + H^+ \rightarrow H_2CrO_4 \qquad (4)$$

The rate of the complex formation decreased as the formation of H_2CrO_4 took place. Therefore, the % removal efficiency of the ELM decreased.

- The other reason for a decrease in the final % removal efficiency can be given as an increase in the osmotic pressure due to a large pH difference between the feed phase and the internal phase. An increase in the osmotic pressure increased the swelling of the membrane during the extraction process. Eventually, the membrane ruptured and the recovered Cr diffused in the feed phase and the final % of Cr removal decreased.

From the above discussion it can be concluded that after attaining an optimum value (0.5 for this study) the % removal decreases with a decrease in pH. Similar results were also reported by Strzelbicki et al. (1984) during extraction of Cr from sulphuric acid solutions with Aliquat 336.

Hence, an initial pH value of 0.5 was kept for all the forthcoming experiments.

4.2.7. Effect of internal to membrane phase ratio

Internal to membrane phase ratio (I/O) is termed as the ratio of the volume of internal phase to the volume of membrane phase. An optimized value of this ratio is necessary in order to get a stable and productive ELM. It is necessary to mention here that the change of W/O emulsion to O/W emulsion is highly dependent on the relative volume of the internal, the membrane phase, HLB number of the system and temperature. The phase inversion caused by the change in the relative volume of the internal and the membrane phase is referred as catastrophic phase inversion.

If the internal phase volume exceeds the maximum value, either the membrane breaks or the phase inversion takes place. In both cases, there is a decrease in the final removal efficiency.

The effect of the internal to membrane phase ratio is shown in Fig. 4.15. Phase ratio was varied in the range of 1/4 to 1. The membrane phase volume was kept constant and the internal phase volume was changed in order to obtain the desired phase ratio. It was found out that an increase in the phase ratio from 1/4 to 1/3 enhanced the % removal efficiency of the ELM by about 8%. This may be due to the fact that the number of stripping molecules increased which enhanced the stripping rate at the inner interface. Hence, Cr concentration in the internal phase increased. Another reason for the enhanced recovery can be proposed as the increment in the number of internal droplets which were widely and densely distributed in the emulsion globules and are easily accessible for the stripping reaction. The thickness of the walls of the membrane globule decreased when the phase ratio is increased. As a result, the complex travelled relatively less in distance between the two interfaces. Hence, the overall efficiency increased.

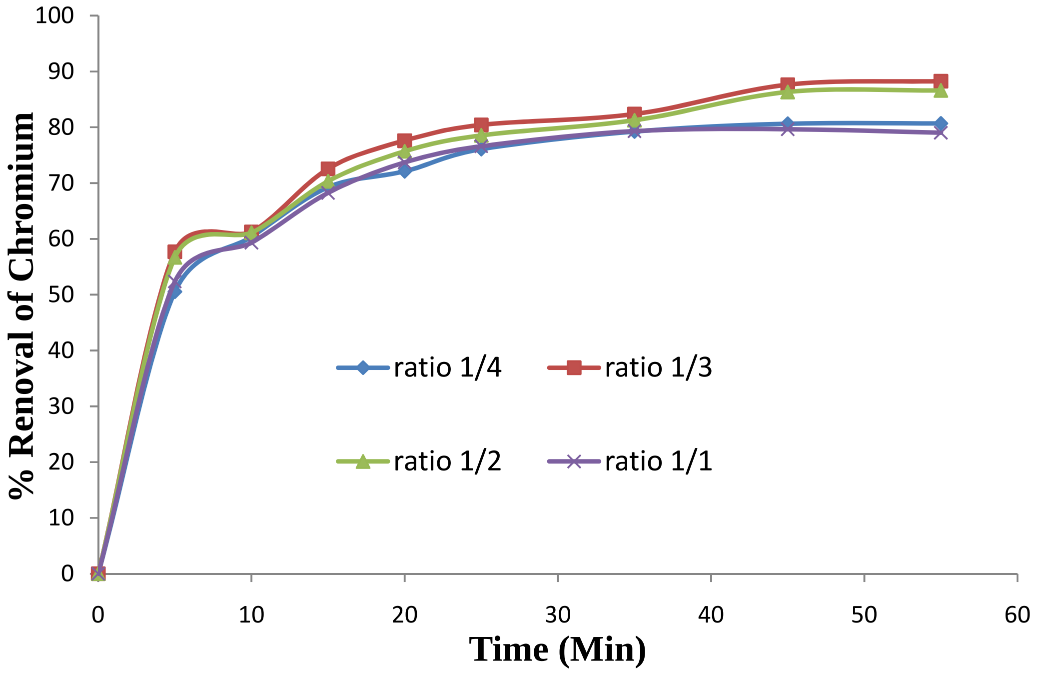

Figure 4.15 The effect of internal to membrane phase ratio. [NaOH] = 0.1 M; Span 80 = 3 %(w/w); [TOMAC] = 0.3 %(w/w); $[BMIM]^{+}[NTf_2]^{-}$= 3 %(w/w); agitation speed = 300 rpm; F/E = 2:1.

However, when the phase ratio was increased from 1/3 to 1/2 and finally to 1, a decrease in the system efficiency was observed. It can be noticed from Fig. 4.15 that the system efficiency drops lesser for a change from 1/3 to 1/2 than from 1/2 to 1. The drop in the ELM efficiency can be explicated by the following reasons:

- As the phase inversion has been discussed earlier in this section, the phase inversion tendency increased upon increasing increase the volume of the internal phase. It can be concluded that the change in phase ratio from 1/3 to 1/2 initiates the phase conversion process and it became apparent when the ratio was further increased from 1/2 to 1. As a result, system efficiency was reduced.

- When volume of internal phase (NaOH) was increased, the effective concentration of NaOH in the emulsion increased as the volume of the membrane phase is fixed. This promoted the interaction of NaOH and Span 80. Consequently, the properties of Span 80 molecules were changed that caused a reduction in the stability of the ELM and the system recovery slimmed down (Kumbasar, 2009).
- Since NaOH concentration increment reduced the viscosity of the membrane, the stability reduced and mass transfer resistance decreased. From the results, it may be concluded that the loss of system recovery due to emulsion stability was more predominant than the increase in the system recovery due to the decrease in mass transfer resistance (Chakrabarty et al., 2010).

Nonetheless, the effect of phase ratio on the % removal efficiency of ELM process varies with the composition and the ingredients of the ELM. It depends on the interactions between molecules, physical properties of each component, HLB number of the system and temperature. Therefore, a 1/3 phase ratio was selected as an optimum value for this ELM system.

4.2.8. Effect of homogenizer speed in emulsification

Homogenization is a process by which aqueous phase is poly-dispersed in organic phase. The size of the dispersed droplets is dependent on the speed of the homogenizer. As the speed increases, the size of the droplets decreases which means that the surface area of the droplets increases, hence, mass transfer rate increases during the extraction (Hanna and Larson, 1985). Hsu and Li (1985) suggested that coalescence is a very sensitive function of droplet size and the ease of coalescence is reduced greatly by reduction in droplet size.

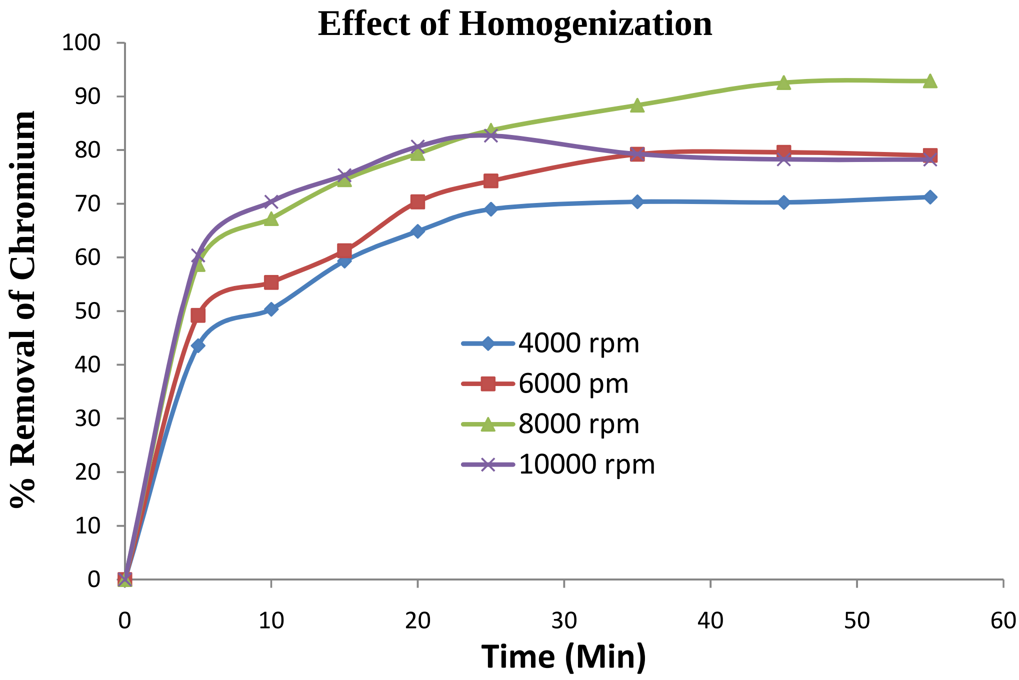

Figure 4.16 The effect of homogenization speed. [NaOH] = 0.1 M; Span 80 = 3 %(w/w); [TOMAC] = 0.3 %(w/w); $[BMIM]^+[NTf_2]^-$= 3 %(w/w); I/O = 1:3 agitation speed = 300 rpm; F/E = 2:1.

The purpose of this study was to investigate the effect of various emulsification processes which was differentiated by their homogenizer speed. Homogenization speed of the emulsification was varied in the range of 4000 - 10000 rpm and the results are as depicted in Fig. 4.16. It can be observed from the figure that an increase in the homogenizer speed increases the % removal due to the formation of smaller internal droplets which occurs at a high homogenizer speed. The available surface area for the extraction reaction increases and more Cr-TOMA or Cr-TOMA complexes were stripped at the inner interface. This trend was found up to a value of 8000 rpm.

Further increase in the homogenizer speed reduces the % removal of Cr as shown in Fig. 4.16. At 10000 rpm, the removal follows the same trend as for previous speeds but after 25 minutes, a sudden decrease in the % removal was observed. This abrupt change was believed to be the effect of the increased swelling caused by the heavy transportation of water molecules from the phase. An increment in the surface area of internal droplets not only increased the mass transfer of the Cr-TOMA complexes but it increased the mass transfer of water molecules too. The volumes of internal droplets kept on increasing until they busted out and the stripped Cr diffused back to the feed phase to nullify the extraction process.

Finally, it can be concluded that homogenization speed is as equally important as agitation speed. The best homogenizing speed to get the maximum removal efficiency was found to be 8,000 rpm.

4.3. Statistical optimization and modelling using response surface methodology

Response surface methodology (RSM) has attracted a substantial deal of interest in the past few decades. It is a statistical tool which is commonly used to optimize the parameters of experiment, to model and to analyze a response of interest. RSM not only provides an optimum level for each variable but also estimates interactions among them and their impact on one or more measured responses. This methodology cuts down the number of experiments substantially without affecting the interactions among the parameters. RSM has been utilized to optimize the parameters of several biotechnological processes such as fermentation, biosorption of metals, oxidation and catalyzed reaction conditions (Kristo et al., 2003; Lai et al., 2003; Soo et al., 2004). It has also been a useful tool to optimize widely employed parameters such as temperature, pH, stirring speed, concentration of various phases and aeration rate in several processes (Mannan et al., 2007; Nosrati et al., 2010; Rajasimman and Sangeetha, 2009; Rajasimman et al.,2009). Hence, the same was applied for the statistical optimization of the parameters such as homogenization speed, carrier concentration, internal phase concentration, agitation speed, treat ratio, internal to membrane phase ratio, surfactant concentration and pH of the feed phase to study the individual and interactive effects of the parameters on the extraction of Cr using ELM. The optimized values were compared with the values obtained from the experimental work described in Section 4.2.

Design-Expert 7.16 software was used to analyze the data and to estimate the coefficients of the regression equation. An orthogonal 2^4 Box-Behnken design (BBD) having five replicates at the centre point was used to estimate the coefficients of the response function which is a second order polynomial as given by equation 5. It resulted in 29 experiments for four variables.

$$Y = \beta_0 + \sum_{i=1}^{k} \beta_i X_i + \sum_{i=1}^{k} \beta_i X_i^2 + \sum_{i_{i<j}}^{k} \sum_{j}^{k} \beta_{ij} X_i X_j + \cdots + e \qquad (5)$$

where Y is the predicted response, β_i, β_j, and β_{ij} are coefficients estimated from the regression, X_i is the uncoded value of the i^{th} variable. i is the linear coefficient, j is the quadratic coefficient, k is the number of factors and e is the random error.

Due to the large number of variables, two sets of four variables each were formed and described as following:

Set - I	Set - II
Homogenization speed (rpm), X_1	pH of the feed phase, X_5
Internal phase concentration (% w/w), X_2	Agitation speed (rpm), X_6
Carrier concentration (% w/w), X_3	Treat ratio, X_7
Surfactant concentration (% w/w), X_4	Internal to Organic phase ratio, X_8

The coded and uncoded values, different levels and the range of the variables are given in Table 4.4.

Table 4.4: Factors and their corresponding values.

Factors	Levels		
	-1	0	1
Homogenization speed (rpm), X_1	4000	7000	10000
Internal phase concentration (% w/w), X_2	0.05	0.525	1
Carrier concentration (% w/w), X_3	0.1	0.3	0.5
Surfactant concentration (% w/w), X_4	1	3	5
pH of the feed phase, X_5	0.2	1.1	2
Agitation speed (rpm), X_6	100	250	400
Treat ratio, X_7	1	2	3
Internal to organic phase ratio, X_8	0.25	0.625	1

4.3.1. Interactions and optimization of the variables of set-I

Box-Behnken design matrix for the set-I is given in Table 4.5 along with the experimental and the predicted response. The percentage removal efficiency of Cr was considered as the predicted response in DoE. Experiments were conducted in the same sequence as they are provided in the Table 4.5 and 4.7 while keeping all other four variables at constant values. The pH of the feed phase was maintained at 0.5 while an agitation speed of 300 was fixed to achieve the maximum surface area. The treat ratio (F/E) and internal to organic phase ratio (I/O) were kept at a value of 2 and 1/3, respectively. The methodology of the experiments was kept similar to the one described in Chapter 3.

The corresponding coefficients of Equation 5 for this set were obtained by regression analysis of the experimental data, and the equation in decoded form is shown in Equation 6. In the equation, only the significant variables are included.

$$Y = 93.59 + 0.95*X_1 + 2.76*X_3 + 0.57*X_4 - 3.80*X_1^2 - 7.46*X_2^2 \qquad (6)$$

$$-8.08*X_3^2 - 10.07*X_4^2 + 2.36*X1*X_2 + 0.81*X_1*X_3 + 3.88*X_1*X_4$$

$$+4.56*X_2*X_3 - 2.87*X_3*X_4$$

where Y is the percentage removal efficiency of Cr by ELM, X_1 is the homogenization speed, X_2 is the internal phase concentration, X_3 is the carrier concentration and X_4 is the surfactant concentration. The predicted values calculated from Equation 6 were in agreement with the experimental values as shown in Fig. 4.17. Hence, this quadratic model was well suited for this experimental set up.

The significance and the fitness of the model was verified by using a widely known statistical test which is ANOVA (Analysis of Variance). ANOVA also facilitates the objective of checking the validity of the equation. The ANOVA results are illustrated in Table 4.6.

Table 4.5: Box-Behnken design matrix for set-I.

Run	X_1	X_2	X_3	X_4	% Removal of Cr	
					Experimental	Predicted
1	0	-1	0	-1	75.56	75.90
2	-1	0	0	-1	74.34	74.33
3	0	0	0	0	93.86	93.59
4	-1	-1	0	0	84.56	83.91
5	0	0	0	0	93.43	93.59
6	0	0	0	0	93.44	93.59
7	0	0	1	1	76.45	75.91
8	1	0	0	-1	83.76	84.00
9	-1	0	1	0	82.45	82.72
10	0	-1	-1	0	80.43	80.02
11	-1	0	0	1	83.54	83.22
12	0	0	0	0	93.3	93.59
13	-1	1	0	0	78.61	78.86
14	1	0	0	1	77.45	77.37
15	1	-1	0	0	81.63	81.11
16	0	-1	1	0	76.32	76.43
17	0	-1	0	1	75.43	76.57
18	0	1	0	-1	75.89	75.11
19	0	0	-1	1	76.34	76.12
20	-1	0	-1	0	78.34	78.81
21	1	0	-1	0	79.01	79.10
22	0	1	-1	0	70.76	70.57
23	1	1	0	0	85.1	85.48
24	0	1	0	1	76.67	76.69
25	0	0	-1	-1	68.98	69.25
26	0	1	1	0	84.89	85.21
27	1	0	1	0	86.35	86.24
28	0	0	1	-1	80.56	80.51
29	0	0	0	0	93.94	93.59

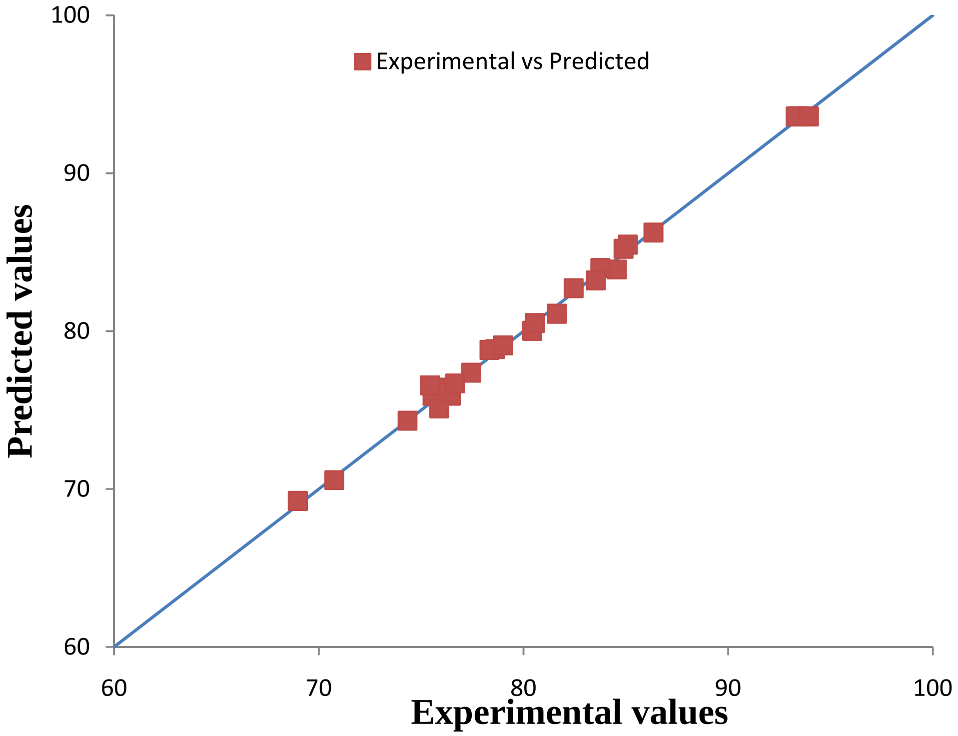

Figure 4.17 Predicted vs experimental values for set-I.

The Model F-value of 304.56 implies that the model is significant. There is only a 0.01% chance that a Model F-Value this large could occur due to noise. Values of Prob > F less than 0.0500 indicate that the model terms are significant and the rest are considered as insignificant. In this case X_1, X_3, X_4, X_1^2, X_2^2, X_3^2, X_4^2, X_1X_2, X_1X_3, X_1X_4, X_2X_3, X_3X_4 are significant model terms. Values greater than 0.1000 indicate the model terms are not significant. The Lack of Fit F-value of 5.08 implies that it is not siginificant in comparison with the pure error. There is a 6.56% chance that a Lack of Fit F-value this large could occur due to noise. It is always necessary to have the value of Lack of Fit F-value to be non significant to make the model best fit.

Predicted R^2 represnts the prediction of a respose value estimated by the model. The difference between adjusted R^2 and predicted R^2 should be in the range of 0-0.200 for the adequacy of the model. In this case, the differecne between them is 0.0113 which implies that the values are in good agreement.

Adequate precision is an estimation of the signal to noise ratio. A ratio greater than 4 is desirable. The ratio of 59.787 implies an adequate signal. Hence, this model can be used to navigate the design space. The coefficient of variation indicates the error expressed as a percentage of the mean.

Table 4.6: ANOVA for response surface model of set-I.

Source	Sum of squares	DF	Mean Square	F-Value	P-Value, prob>F	
Model	1366.76	14	97.63	304.56	< 0.0001	significant
X_1	10.94	1	10.94	34.14	< 0.0001	
X_2	0.34	1	0.34	1.05	0.3228	
X_3	91.63	1	91.63	285.86	< 0.0001	
X_4	3.84	1	3.84	11.99	0.0038	
X_1^2	93.52	1	93.52	291.74	< 0.0001	
X_2^2	360.81	1	360.81	1125.63	< 0.0001	
X_3^2	423.43	1	423.43	1320.96	< 0.0001	
X_4^2	657.53	1	657.53	2051.30	< 0.0001	
X_1X_2	22.18	1	22.18	69.21	< 0.0001	
X_1X_3	2.61	1	2.61	8.14	0.0128	
X_1X_4	60.14	1	60.14	187.62	< 0.0001	
X_2X_3	83.17	1	83.17	259.48	< 0.0001	
X_2X_4	0.21	1	0.21	0.65	0.4350	
X_3X_4	32.89	1	32.89	102.61	< 0.0001	
Residual	4.49	14	0.32			
Lack of Fit	4.16	10	0.42	5.08	0.0656	not significant
Pure Error	0.33	4	0.082			
Cor Total	1371.25	28				

Std. deviation = 0.57; mean = 81.43; Coefficient of variation = 0.70; R-squared = 0.9967; Adjusted R-squared = 0.9935; Predicted R-squared = 0.9822; Adequate precision = 59.787

The response surface curves indicate the interaction of the variables and also determine the optimum level of variables for maximum response. The response surface plots for significant interaction between two variables against % removal efficiency of Cr by the ELM are shown in Figs. 4.18, 4.19, 4.20, 4.21 and 4.22.

4.3.1.1. Significant interactions of the variables of set-I

The contour plot in Fig. 4.18 illustrates the interaction between the homogenization speed and the internal phase concentration/NaOH concentration. In the figure, the parabolic nature of contours implies that the interaction between both variables is significant. The homogenization speed and the internal phase concentration caused an increase in the % removal efficiency when their values were increased from a lower level to up to a certain point. After this point, the % removal efficiency decreases, as illustrated in Fig. 4.18. The optimized values are provided in Section 4.3.1.2.

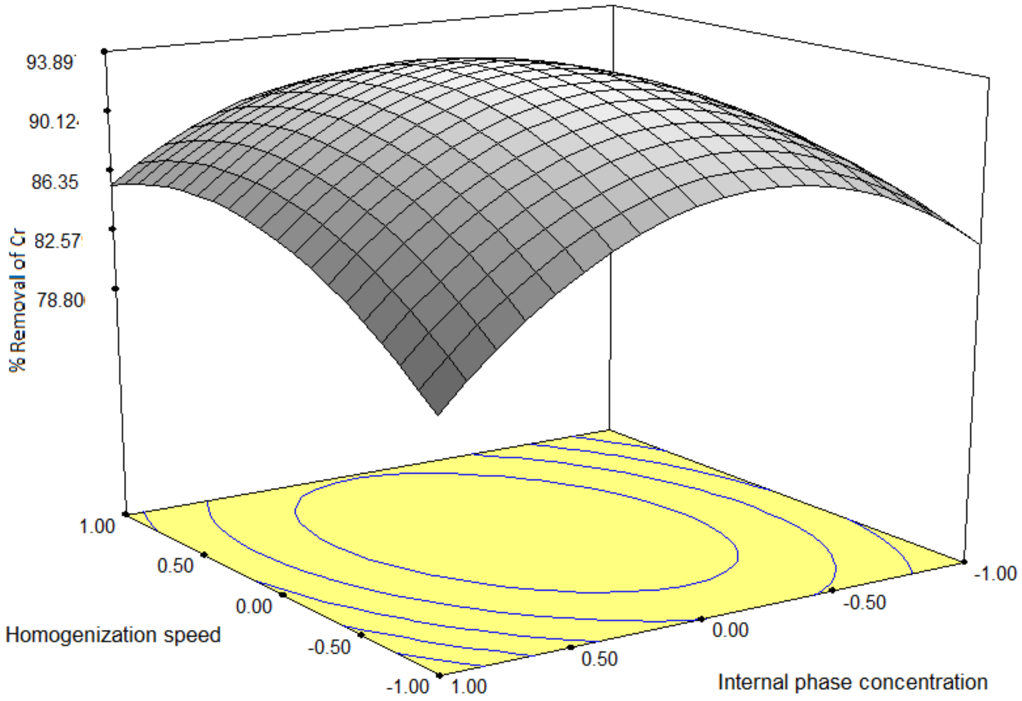

Figure 4.18 Response surface plot for the interaction between the homogenization speed and the internal phase concentration.

The interaction between the homogenization speed and the internal phase concentration can be explained by the fact that the viscosity is directly proportional to the internal phase concentration and the internal phase droplet size is dependent on the viscosity and the homogenization speed. Thus, they are interrelated.

The interaction between the homogenization speed and the carrier concentration is shown in Fig. 4.19. Parabolic contours signify that the interaction between them is significant. The viscosity of the ELM is dependent on the carrier concentration and the small sized globules formation is dependent on the viscosity and homogenization speed. The curve illustrates that the % removal efficiency increases upon increasing both the values from lower level but, after reaching optimum values of .32% (w/w) and 7430 rpm removal efficiency tend to decline up to the higher level. The optimum values can be easily determined since the contours are parabolic. TOMAC increased the viscosity of the ELM and reduced the effect of homogenization speed.

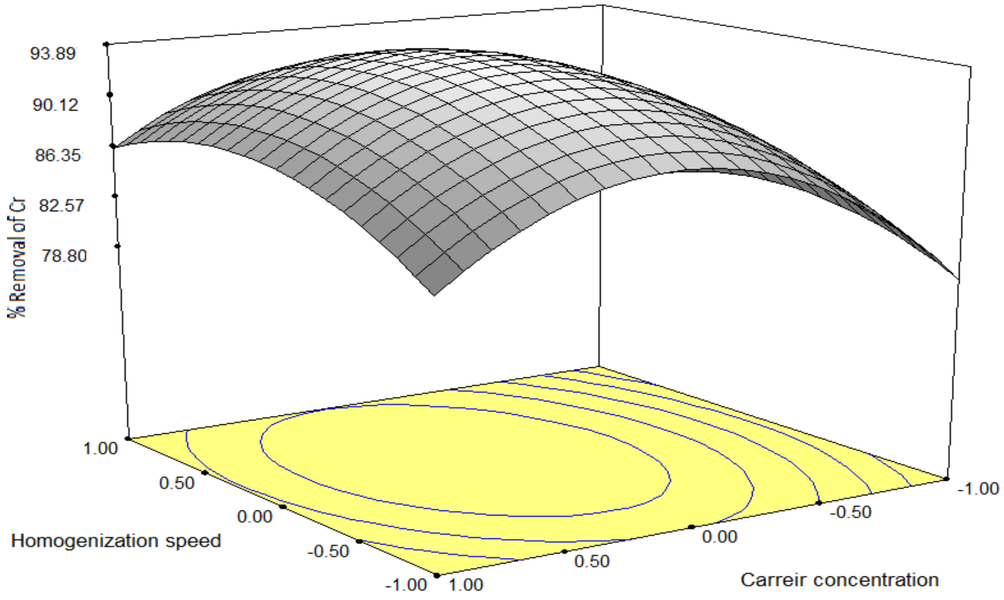

Figure 4.19 Response surface plot for the interaction between homogenization speed and the carrier concentration.

Figure 4.20 demonstrates the interaction between the homogenization speed and the surfactant concentration. The % removal of Cr increases upon increasing the concentration of Span 80 up to a value of 2.85% (w/w). However, it decreases after a further increment in Span 80 concentration up to the higher level. A similar kind of results was obtained for the homogenization speed. It means that both are having optimum values at which maximum % removal can be achieved. Since the contours are parabolic, interaction between homogenization speed and Span 80 concentration is significant. The reason for the significant interaction can be given as the protecting nature of the surfactant which helps to protect the internal droplets from high shear and stress caused by the homogenization speed. Surfactant concentration also contributes in generating fine droplets in the internal phase under a reasonable homogenization speed.

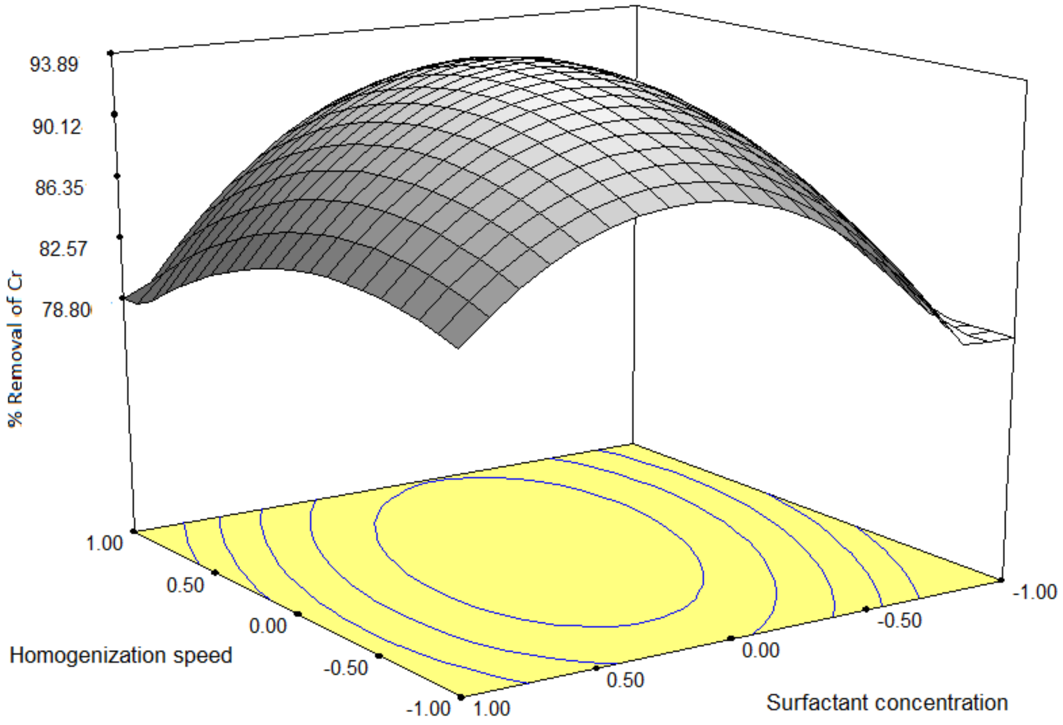

Figure 4.20 Response surface plot for the interaction between the homogenization speed and the surfactant concentration.

The interaction between the internal phase concentration and the carrier concentration is illustrated in Fig. 4.21. The contours are parabolic, indicating that the interaction is significant. The % removal of Cr increases upon increasing both parameters from the lower range up to optimum values of 0.52M and 0.32% (w/w) of internal phase concentration and carrier concentration, respectively. After optimum values have been reached, the % removal of Cr decreases. The interaction can be interpreted physically as the reaction between TOMAC and NaOH which takes place at the inner interface. The reaction not only affects the stripping reactions but also the overall removal efficiency. Another important interaction between them can be given as the involvement of carrier and the internal phase in the extraction and stripping reaction, respectively. Hence, they are highly interactive parameters in the ELM process.

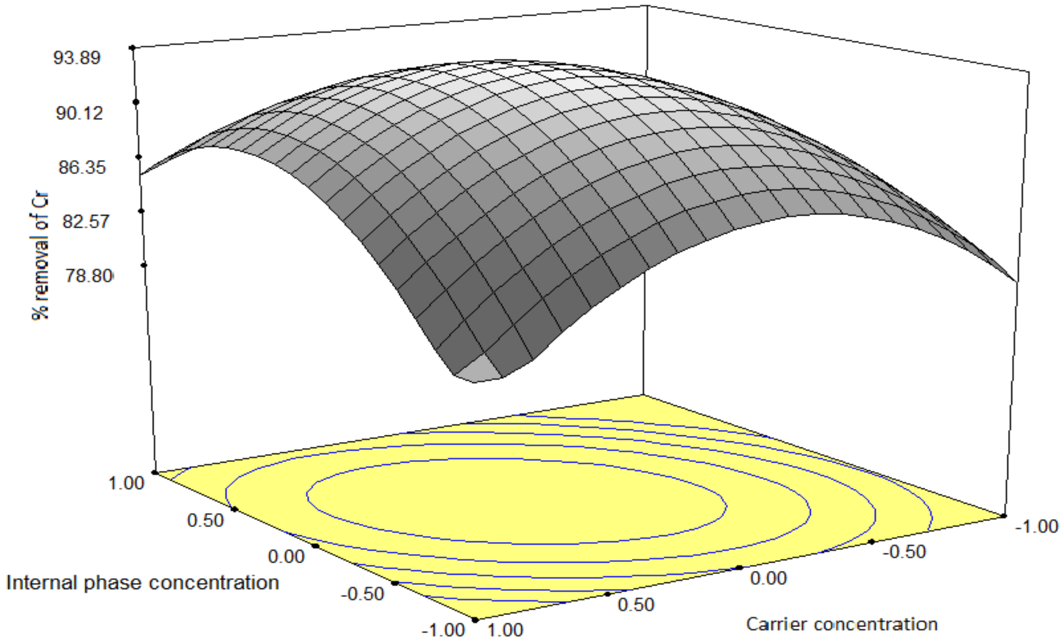

Figure 4.21 Response surface plot for the interaction between the internal phase concentration and the carrier concentration.

Fig. 4.22 shows the interaction between the carrier concentration and the surfactant concentration. Circular contours imply that the interaction between the parameters is not significant. Hence, the optimum values of the variables are not easy to determine. However, increasing the surfactant concentration and carrier concentration increases the % removal efficiency up to optimum values of 2.9% (w/w) and 0.32% (w/w) of Span 80 concentration and TOMAC concentration, respectively. The removal efficiency decreases upon further increment of both values. The trend of the curve is more or less similar to the ones described earlier for other variables' interactions except the contours.

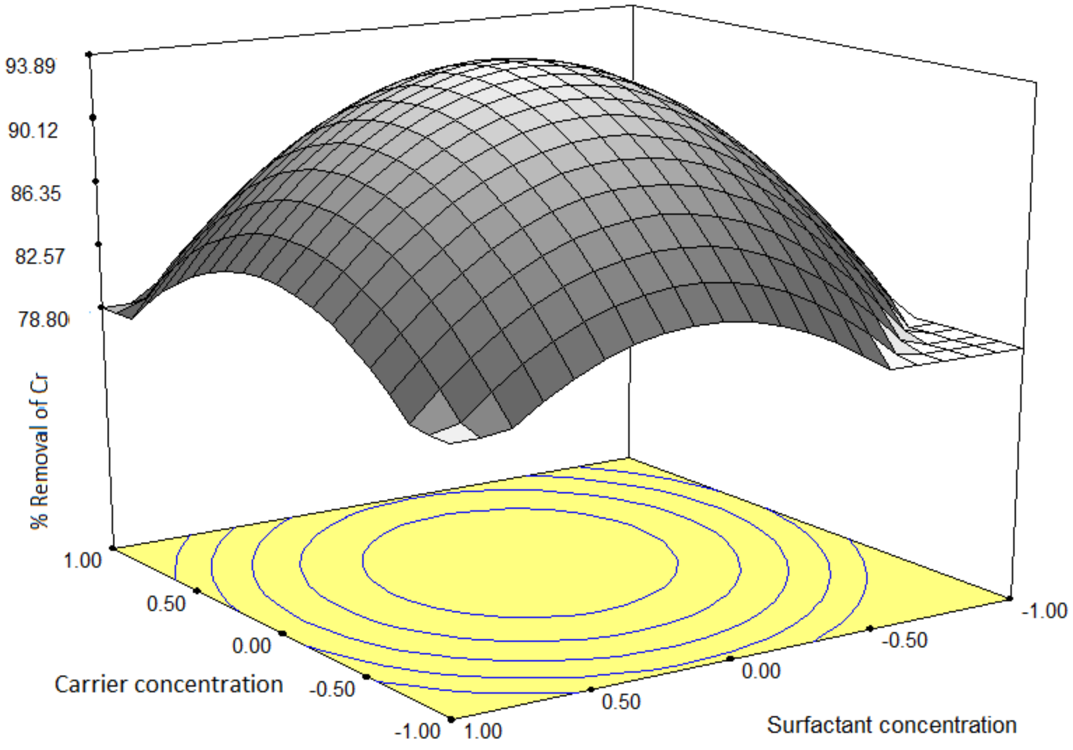

Figure 4.22 Response surface plot for the interaction between the carrier concentration and the surfactant concentration.

4.3.1.2. Optimization of the variables of set-I

The statistical optimization of all four parameters was accomplished by Design of Experiments (DoE) 7.04. DoE resulted in 10 different solutions having almost the same % removal of Cr. The solution with the minimum carrier concentration was selected as the carrier was the most expensive amongst the chemicals used. The coded values of the homogenization speed, the internal phase concentration, the carrier concentration and the surfactant concentration are 0.22, 0.05, 0.18 and -0.03, respectively. The % removal efficiency was predicted at a value of 93.94% under these optimized values. The uncoded values for the homogenization speed and the internal phase concentration were calculated from the coded values and they were 7660 rpm and 0.548M, respectively. Similarly, the carrier concentration and the surfactant concentration were 0.336 and 3.06 % (w/w), respectively.

All the optimum values were in good agreement with the experimental optimization, as described in Section 4.2, except for the value of the internal phase concentration. The reason for this discrepancy can be attributed to the large value range chosen (0.05 -1M) for the internal phase concentration. However, the model results are significant and well suited to the experimental results.

4.3.2. Interactions and optimization of the variables of set-II

Similarly, Box-Behnken design matrix for set-II was obtained by DoE 7.04 and is given in Table 4.7. The experiments were conducted in the sequence illustrated in the table, keeping all other four variables at the constant optimized values predicted by Set-I analysis. The homogenization speed was maintained at 7660 rpm while the internal phase concentration at a value of 0.548 M was fixed so as to achieve the optimum stripping reagent. The respective carrier concentration and the surfactant concentration were taken as 0.336 and 3.06 %(w/w), and experimental methodology was similar to the one described in Section 3.2.

The corresponding coefficients for Equation 5 for this set were obtained by regression analysis of the experimental data and the equation in decoded form is as shown in Equation 7. In this equation, insignificant terms are discarded and only significant terms have been included.

$$Y = 94.49 - 16.44*X_5 + 3.33*X_6 + 4.25*X_7 - 18.94*X_5^2 - 8.51*X_6^2 - 8.55*X_7^2 - 6.50*X_8^2 - 3.10*X_5*X_6 + 4.78*X_7*X_8 \qquad (7)$$

where Y is the percentage removal efficiency of Cr by the ELM, X_5 is the pH of the feed phase, X_6 is the agitation speed, X_7 is the treat ratio and X_4 is the internal to membrane phase ratio. The predicted values calculated from Equation 7 were in very good agreement with the experimental values, as shown in Fig. 4.22. Thus, this quadratic model is well suited for this experimental set-up.

Furthermore, the validation and the fitness of the model were affirmed by ANOVA. The ANOVA results are as shown in Table 4.8.

Table 4.7: Box-Behnken design matrix for set-II.

Run	X_1	X_2	X_3	X_4	% Removal of Cr	
					Experimental	Predicted
1	-1	0	0	1	85.43	87.20
2	0	0	0	0	94.69	94.49
3	0	-1	-1	0	69.45	68.97
4	1	-1	0	0	50.23	50.36
5	0	-1	0	-1	73.48	75.13
6	0	0	1	1	89.92	89.02
7	1	1	0	0	48.29	50.83
8	0	0	-1	1	70.69	70.95
9	1	0	0	-1	55.45	53.21
10	0	1	-1	0	78.43	77.38
11	0	0	0	0	95.02	94.49
12	0	0	1	-1	78.43	78.35
13	0	0	0	0	93.7	94.49
14	0	0	0	0	95.32	94.49
15	0	-1	1	0	78.64	79.22
16	-1	-1	0	0	79.41	77.05
17	1	0	-1	0	44.98	44.83
18	0	1	1	0	84.12	84.13
19	1	0	1	0	56.32	56.27
20	0	0	0	0	93.72	94.49
21	0	1	0	1	84.26	82.90
22	-1	0	1	0	85.78	86.22
23	0	-1	0	1	76.68	77.15
24	0	0	-1	-1	78.33	79.41
25	0	1	0	-1	82.89	82.71
26	-1	0	0	-1	84.01	83.78
27	-1	1	0	0	89.87	89.91
28	-1	0	-1	0	80.32	80.66
29	1	0	0	1	52.23	51.99

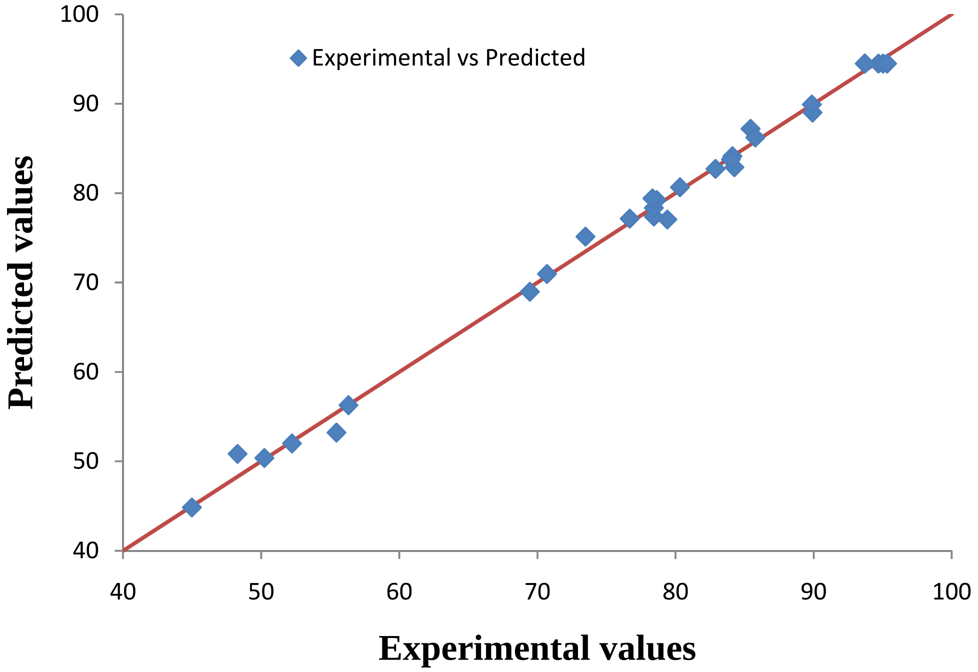

Figure 4.23 Predicted vs experimental values for set-II.

The Model F-value of 202.94 implies that the model is significant. There is only a 0.01% chance that a Model F-Value this large could occur due to noise. Values of Prob > F less than 0.0500 indicate model terms are significant and the rest are considered insignificant. In this case X_5, X_6, X_7, X_5^2, X_6^2, X_7^2, X_8^2, X_5X_6 and X_7X_8 are significant model terms. Values greater than 0.1000 indicate the model terms are not significant. The Lack of Fit F-value of 5.24 implies that it is not significant in comparison with the pure error. There is a 6.22% chance that a Lack of Fit F-value this large could occur due to noise. It is always necessary to have the value of “Lack of Fit F-value” non significant to make the model best fit.

Table 4.8: ANOVA for the Response surface model of set-II.

Source	Sum of squares	DF	Mean Square	F-Value	P-Value, prob>F	
Model	6374.46	14	455.32	202.94	< 0.0001	significant
X_5	3244.60	1	3244.60	1446.14	< 0.0001	
X_6	133.13	1	133.13	59.34	< 0.0001	
X_7	216.84	1	216.84	96.64	< 0.0001	
X_8	3.65	1	3.65	1.63	0.2228	
X_5^2	2326.86	1	2326.86	1037.10	< 0.0001	
X_6^2	469.89	1	469.89	209.43	< 0.0001	
X_7^2	474.59	1	474.59	211.53	< 0.0001	
X_8^2	274.48	1	274.48	122.34	< 0.0001	
X_5X_6	38.44	1	38.44	17.13	0.0010	
X_5X_7	8.64	1	8.64	3.85	0.0699	
X_5X_8	5.38	1	5.38	2.40	0.1437	
X_6X_7	3.06	1	3.06	1.36	0.2622	
X_6X_8	0.84	1	0.84	0.37	0.5511	
X_7X_8	91.49	1	91.49	40.78	< 0.0001	
Residual	31.41	14	2.24			
Lack of Fit	29.18	10	2.92	5.24	0.0622	not significant
Pure Error	2.23	4	0.56			
Cor Total	6405.87	28				

Std. deviation = 1.50; mean = 76.90; Coefficient of variation = 1.95; R-squared = 0.9951; Adjusted R-squared = 0.9902; Predicted R-squared = 0.9732; Adequate precision = 46.096

Predicted R^2 represents the prediction of a respose value estimated by the model. The difference between adjusted R^2 and predicted R^2 is desired to be in the range of 0-0.200 for the adequacy of the model. In this case, the differecne between them is 0.0173 which implies that both the values are in good agreement.

Adequate precision is an estimation of the signal to noise ratio. A ratio greater than 4 is desirable. The ratio of 46.096 implies an adequate signal. Hence, this model can be used to navigate the design space. The coefficient of variation indicates the error expressed as a percentage of the mean.

4.3.2.1. Significant interactions of the variables of set-II

There were only two significant interactions for set-II, as previously shown by ANOVA. These were: (i) interaction between the pH of the feed phase and the agitation speed, and (ii) interaction between the treat ratio and the internal to membrane phase ratio. The response curves of both are as shown in Figs. 4.23 and 4.24, respectively.

In Fig. 4.24, the contours of the curve are parabolic, implying the interaction between pH of the feed phase and agitation speed is significant and the optimum values can easily be calculated. The % removal of Cr increases upon decreasing the pH of the feed phase but, after an optimum value of 0.412, the removal of Cr decreases with a further decrease in the pH. A similar trend can also be observed for the agitation speed. This implies that both have specific optimum values, and therefore maximum removal of Cr can be achieved

The interaction between the pH of the feed phase and the agitation speed can be explained by the fact that swelling in ELM is caused by the pH of the feed phase and by the agitation speed. Extraction rate increases upon increasing the agitation speed, which reduces the pH difference between the internal phase and the feed phase. This process influences swelling by a significant amount. Hence, swelling acts as a connecting parameter to influence the interaction between them. The other connecting parameter can be attributed as osmotic pressure difference between the internal and the feed phase which is dependent on the pH of the feed phase and the agitation speed.

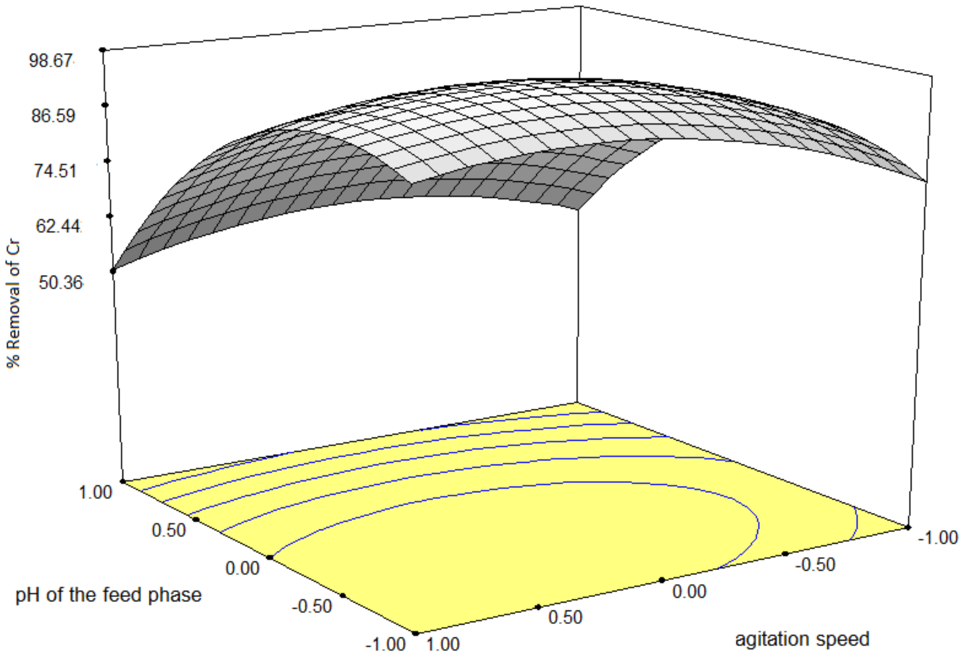

Figure 4.24 Response surface plot for the interaction between the pH of the feed phase and the agitation speed.

Fig. 4.25 shows the interaction between the treat ratio and the internal to membrane phase ratio. Parabolic contours signify that the interaction is quite significant. The figure predicts that the increment in the treat ratio increases the % removal of Cr through this range while internal to membrane phase ratio achieves a maxima in between the range. The possible reason for the interaction can be provided as the direct proportionality of the internal to membrane phase ratio to the treat ratio.

An increment in the internal to membrane phase ratio increases the volume of the ELM which in turn decreases the treat ratio. Therefore, they have a good interaction for the ELM process.

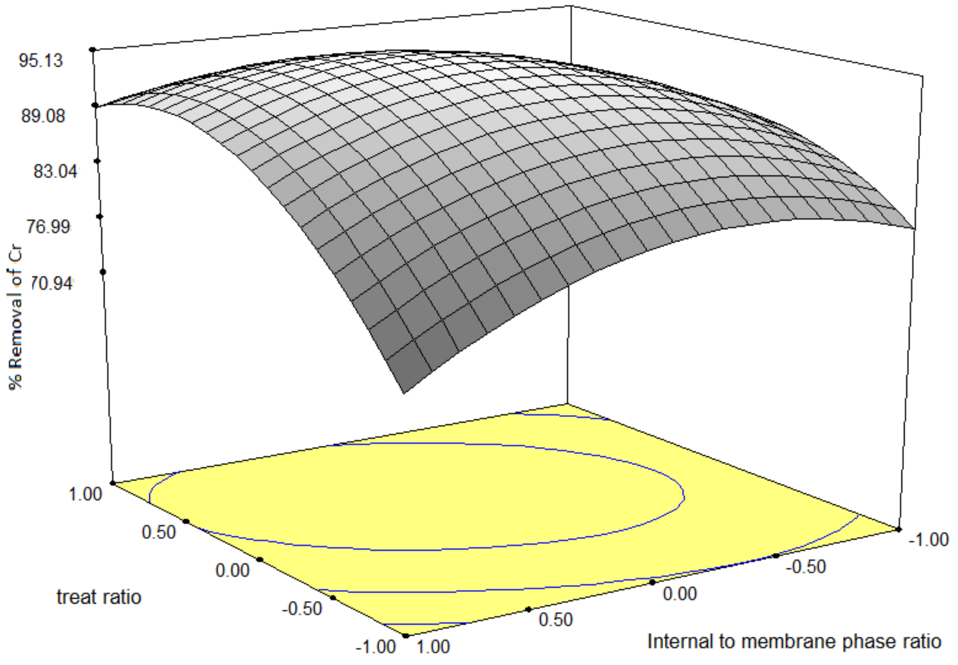

Figure 4.25 Response surface plot for the interaction between the treat ratio and the internal to membrane phase ratio.

4.3.2.2. Optimization of the variables of set-II

The statistical optimization of all four parameters was accomplished by Design of Experiments (DoE) 7.04. DoE resulted in 10 different solutions having the % removal of Cr up to 97.5. However, the solution with the maximum treat ratio has been selected to economize the ELM process. The coded values of the pH of the feed phase, the agitation speed, the treat ratio and the internal to membrane phase ratio were -0.75, 0.31, 0.60 and 0.24, respectively. Using these optimized values, the % removal efficiency was predicted at 96.38%. The uncoded values for the pH of the feed phase and the agitation speed were calculated from the coded values, and they were 0.425 and 296.5rpm, respectively.

Likewise, through the conversion of coded values to uncoded values the treat ratio and the internal to membrane phase ratio were found to be 2.60 and 0.715, respectively.

All the above optimum values are in good agreement with the experimental optimization, as described in Section 4.2, except for the value of the treat ratio. However, the results of the model are significant and well suited to the experimental results.

Table 4.9 provides a comparison of the optimized values calculated experimentally and by the RSM. It shows that all the values are in good agreement except for the internal phase concentration and the treat ratio. This difference is dependent on the range and levels defined for the RSM, swelling of the ELM and other experimental errors. However, the model can be used to predict the % removal of Cr by the ELM.

Table 4.9: Comparison of experimentally optimized values and RSM optimized values.

Parameter	Exptt. optimized	RSM optimized	ǀErrorǀ
Homogenization speed (rpm)	8000	7660	0.04
Internal phase concentration (M)	0.1	0.548	4.48
Carrier concentration (% w/w)	0.3	0.336	0.12
Surfactant concentration (% w/w)	3.0	3.06	0.02
pH of the feed phase	0.5	0.425	0.15
Agitation speed (rpm)	300	296.5	0.11
Treat ratio	2	2.60	0.30
Internal to membrane phase ratio	0.337	0.715	1.12